

Optimal Deadrise Hull Analysis and Design Space Study of  
Naval Special Warfare High Speed Planing Boats

by

Todd E. Whalen

B.S. Mechanical Engineering, University of Virginia, 1995

Submitted to the Departments of Ocean Engineering and Civil and Environmental Engineering  
in partial fulfillment of the requirements for the degrees of

Master of Science in Naval Architecture and Marine Engineering  
and  
Master of Science in Civil and Environmental Engineering

at the  
Massachusetts Institute of Technology  
June 2002

© 2002 Todd E. Whalen  
All rights reserved

The author hereby grants MIT permission to reproduce and to  
distribute publicly paper and electronic copies of this thesis document in whole or in part.

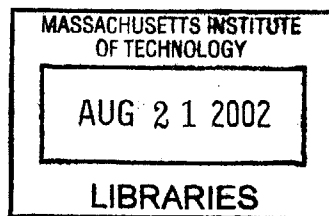
Author .....  
Department of Ocean Engineering  
May 10, 2002

Certified by .....  
J. Kim Vandiver  
Professor of Ocean Engineering  
Thesis Supervisor

Certified by .....  
E. Kausel  
Professor of Civil and Environmental Engineering  
Thesis Supervisor

Accepted by .....  
Oral Buyukozturk  
Professor of Civil and Environmental Engineering  
Chairman, Departmental Committee on Graduate Studies

Accepted by .....  
Henrik Schmjdt  
Professor of Ocean Engineering  
Chairman, Departmental Committee on Graduate Studies



**BARKER**

# **Optimal Deadrise Hull Analysis and Design Space Study of Naval Special Warfare High Speed Planing Boats**

by  
Todd E. Whalen

Submitted to the Departments of Ocean Engineering and  
Civil and Environmental Engineering  
on May 10, 2002, in partial fulfillment of the  
requirements for the degrees of  
Master of Science in Naval Architecture and Marine Engineering  
and  
Master of Science in Civil and Environmental Engineering

## **Abstract**

United States Navy SEALs (Sea, Air, Land) frequently employ high speed planing boats (HSPBs) in the performance of their missions. Operation of these vessels in normal and adverse conditions exposes personnel to severe mechanical shock. Anecdotal evidence and recent medical studies conducted by the Naval Health Research Center show a correlation between HSPB operation and chronic and acute personnel injury. Most current research focuses on short-term solutions that reduce shock at the hull-deck and deck-seat interfaces (deck padding and suspension seats, for example). The object of this thesis is to develop an Optimal Deadrise Hull (ODH) that reduces mechanical shock where it first enters the boat, at the hull-sea interface. Planing boat hydrodynamics were reviewed and the mechanical shock environment was evaluated. The ODH analysis is performed on the MkV Special Operations Craft in order to determine the effects of hull deadrise on vertical acceleration. Finally, the results of the ODH analysis are used to perform a design space study of planing hulls in order to optimize the overall design for vertical acceleration based on hull deadrise, cruise speed, and payload weight.

Thesis Supervisor: J. Kim Vandiver  
Title: Professor of Ocean Engineering

Thesis Reader: E. Kausel  
Title: Professor of Civil and Environmental Engineering

## **Acknowledgements**

First and foremost, I would like to thank my wife, Isabel, and son, Edward, for keeping me sane during these two years and putting up with my monopoly of the home computer. I love you both and I am lost without you. As Edward would say, I am “all fin!”

This thesis would not have been possible without the help of Mr. Richard Akers of Ship Motion Associates. His company donated a copy of its software for use on my project and he took time out of his busy schedule to visit MIT for a much needed information session. To his credit, he never screened his answering machine during any of my repeated calls for help. Professors Kim Vandiver and Eduardo Kausel provided invaluable guidance in the realm of mechanical shock and allowed me to concentrate on my areas of interest. Dr. Cliff Whitcomb coordinated the barrage of email during my topic search and patiently answered all of my questions regarding Response Surface Methods.

# Contents

- Abstract.....2
- Acknowledgements.....3
- Contents .....4
- List of Figures.....5
- List of Tables .....6
- 1 Introduction.....7
  - 1.1 Motivation .....7
  - 1.2 Background .....8
- 2 The Mechanical Shock Environment.....14
  - 2.1 Hydrodynamics of the Hull-Sea Interface.....14
    - 2.1.1 Planing Hull Resistance Summary.....14
    - 2.1.2 Wave Slamming.....17
    - 2.1.3 Vertical Hull Water Entry .....17
  - 2.2 Effects of Mechanical Shock.....18
  - 2.3 Shock Mitigation Concepts .....22
    - 2.3.1 Hull-Sea Interface .....23
    - 2.3.2 Deck-Hull Interface.....26
    - 2.3.3 Seat-Deck Interface.....27
- 3 Optimal Deadrise Hull Analysis.....28
  - 3.1 Design Tool Description .....28
  - 3.2 Design Methodology .....30
  - 3.3 Design Results .....33
- 4 Design Space Study .....36
  - 4.1 Response Surface Methods .....36
  - 4.2 Design Space Creation .....40
  - 4.3 Design Space Analysis .....42
    - 4.3.1 Average Heave Acceleration Response Model.....42
    - 4.3.2 1/3 Highest Heave Acceleration Response .....45
    - 4.3.3 Design Space Case Studies .....47
- 5 Conclusions.....52
  - 5.1 Optimal Deadrise Hull Analysis.....52
  - 5.2 Design Space Study.....53
  - 5.3 Recommendations for Future Work .....53
- Appendix A.....55
- Appendix B.....60
- References.....64

# List of Figures

Figure 1. MkV Special Operations Craft.....	9
Figure 2. Injuries vs. Time in SBUs [14].....	12
Figure 3. Hospitalization Rates [14].....	12
Figure 4. Ship Motion Coordinate Reference [5].....	14
Figure 5. Lift Fraction vs. Froude Number [11].....	15
Figure 6. Free Body Diagram of a Planing Hull [16].....	16
Figure 7. Typical HSPB Shock Event [13].....	18
Figure 8. Effect of Fatigue on Bone and Cartilage Failure [19].....	20
Figure 9. Injury and Discomfort Limits for Repeated Shocks [19].....	21
Figure 10. Design Methods for Shock Mitigation [13].....	22
Figure 11. High Speed Hull Forms [11].....	23
Figure 12. Very Slender Vessel [4].....	24
Figure 13. H-STEP [13].....	25
Figure 14. LocalFlex [14].....	26
Figure 15. Impacting Wedges [1].....	28
Figure 16. MkV SOC Design Model.....	30
Figure 17. Percent Change From Baseline.....	34
Figure 18. Box-Behnken Design.....	39
Figure 19. Central Composite Design.....	40
Figure 20. Average Heave Acceleration Response Model Leverage Plot.....	43
Figure 21. 1/3 Highest Heave Acceleration Response Model Leverage Plot.....	46
Figure 22. Case 1 Heave Acceleration vs. Cruise Speed and Payload.....	48
Figure 23. Case 1 Heave Acceleration Contour Profile.....	49
Figure 24. Case 2 Contour Profile (15 klbs Payload).....	50
Figure 25. Case 2 Contour Profile (30 klbs Payload).....	51

# List of Tables

Table 1. MkV SOC Principal Characteristics .....9  
Table 2. NHRC Survey Participant Characteristics [14] .....10  
Table 3. NHRC Survey Injury Locations [14].....11  
Table 4. Summary of Short-Duration Acceleration Loads [19] .....19  
Table 5. MkV SOC Model Principal Characteristics .....30  
Table 6. Input for Rough Water Simulation .....31  
Table 7. Resistance and Coxswain Heave Acceleration Results .....33  
Table 8. Vertical Acceleration Factor Levels .....41  
Table 9. Central Composite Design Summary .....42  
Table 10. Average Heave Acceleration Response Model Analysis of Variance.....44  
Table 11. Average Heave Acceleration Response Model Coefficients.....45  
Table 12. 1/3 Highest Heave Acceleration Response Model Analysis of Variance.....46  
Table 13. 1/3 Highest Heave Acceleration Response Model Coefficients.....46

# Chapter 1

## Introduction

### 1.1 Motivation

United States Special Forces are comprised of elite combat units from all branches of the US military. In particular, the Naval Special Warfare (NSW) community plays a significant role in projecting national presence and maintaining security around the globe. Navy SEALs (Sea, Air, Land) are tasked with special operations supporting the US Navy and US Special Operations Command (USSOCOM). They provide a broad capacity for special warfare in many environments, ranging from the blue oceans to shores and rivers throughout the world. Typical missions include direct action, special reconnaissance, combating terrorism, counter-drug operations, personnel recovery, and hydrographic reconnaissance [2]. Their mission effectiveness is the result of arduous mental and physical training and depends upon the health of every SEAL and the proper operation of their equipment.

Unlike other military forces, SEALs are maritime Special Forces; they strike from and return to the sea. Special Boat Units (SBUs), one of the major components of the NSW community, are tasked with patrolling the littoral environment and inserting, supporting, and extracting SEALs [2]. High speed planing boats (HSPBs) are routinely used in the performance of these missions, which can occur in both calm water and rough sea states. Operation of these boats subjects both crew and passengers to repeated mechanical shock events due to wave slamming and vertical hull water entry, leading to personnel injury and equipment degradation. The consequences of this shock environment are a reduction in mission effectiveness and the potential for injury to personnel.

Currently, there is no system for shock mitigation on NSW boats. Although the problem has been researched for many years, only minor solutions, such as deck padding, have been incorporated into the boats. Research and development is ongoing in this area, but the focus has shifted to short-term solutions in order to accommodate current operating platforms. However, the most effective shock mitigation system will likely result from a combination of various shock reduction technologies. Improvements in performance by both personnel and equipment will not be realized unless shock reduction methods are developed and implemented effectively. This project investigates a hull geometry solution by determining the effects of hull deadrise on vertical acceleration. Furthermore, a design space is developed in order to evaluate vertical acceleration with respect to other design parameters and examine the combined affects of these factors on shock.

## **1.2 Background**

NSW forces employ many different types of small boats in the performance of their missions. The boat most frequently used by the SBUs is the MkV Special Operations Craft (MkV SOC). Other watercraft, such as the NSW Rigid-Hull Inflatable Boat, River Patrol Boat, Combat Rubber Raiding Craft, and Light Patrol Boat are used by the SBUs but were not evaluated for the purposes of this study. The newer MkV SOC represents the latest in HSPB design and technology; the performance of this craft will determine future designs.

The MkV SOC, shown in Figure 1, is used to carry SEALs into and out of low- to medium-threat coastal environments, support coastal patrol, and interrupt enemy activities. A MkV SOC detachment, which consists of two boats, ten crew, eight maintenance crew, and all associated equipment, can be deployed anywhere in the world within forty-eight hours via C-5 Galaxy cargo aircraft. The MkV SOC is the result of a streamlined acquisition effort managed by USSOCOM that produced the first boat only eighteen months after awarding the contract. The first boat was delivered in 1995, and a total of twenty are currently operational [4].





**Figure 1. MkV Special Operations Craft**

The MkV SOC, which was constructed by Halter Marine Equitable Shipyard, is a high-performance craft capable of speeds in excess of 50 knots. The MkV SOC design improves upon previous Mk III and IV HSPB designs by incorporating technologies such as an Aluminum hull and diesel-waterjet propulsion. The principal characteristics of the MkV SOC are shown in Table 1 [4].

**Table 1. MkV SOC Principal Characteristics**

Length Overall	82 ft	Air/Road Weight Limit	90000 lbs
Maximum Beam	17.5 ft	Installed Power	4570 Hp
Static Draft	5 ft	Max Speed	50+ kts
Depth (Keel to Shear)	7.75 ft	Cruise Speed	35 kts
Lightship Weight	88500 lbs	Range	600+ nm (at 35 kts)
Full Load Displacement	119000 lbs	Crew	5
Payload Capacity	30000 lbs	Passengers	16

As the MkV SOC was being developed, the Navy evaluated its manning of small watercraft and in 1994 developed a new enlisted rating to improve continuity and experience in the small boat community. These new Special Warfare Combat Crewmen (SWCC) were designated to operate and maintain the inventory of high performance boats supporting SEAL missions throughout their entire careers. SWCCs and SEALs go through separate but similar training programs, but SWCCs receive extensive training in

craft and weapons tactics, techniques, and procedures. The SWCCs and the boats they operate provide dedicated, rapid mobility in shallow areas where larger ships cannot operate [2].

Unfortunately, the creation of the SWCC rating only exacerbated existing problem of mechanical shock exposure within the small boat community. Commercial and governmental groups were well aware of the potential for injury while operating HSPBs in calm and rough water conditions, but such injuries were viewed as isolated incidents and not part of a larger problem. Earlier efforts to mitigate injuries due to boat operations were addressed by adjusting operational doctrine and training personnel. Various research efforts studying the causes and possible solutions to mechanical shock on HSPBs were being performed in the early 1990s, but an immediate need for shock mitigating technology was not yet realized.

During the late 1990s, injury of personnel on HSPBs became a more significant problem. Eventually, the Naval Health Research Center (NHRC) performed a study in order to evaluate the severity of the problem. In 1998-99, NHRC personnel administered surveys to 154 personnel from SBU-12, SBU-20, and SBU-22 to determine the prevalence of injuries associated with HSPB operations. Mission logs were reviewed to document new injuries resulting from specific boat operations, and all SWCCs were asked to report circumstances, timing, and nature of past injuries [14]. Table 2 summarizes the participant characteristics of the SWCCs surveyed.

**Table 2. NHRC Survey Participant Characteristics [14]**

<b>Parameter</b>	<b>SBU 12</b>	<b>SBU 20</b>	<b>SBU 22</b>	<b>Total</b>
Respondents	83	43	28	154
Age	32.2 ± 6.1	33.3 ± 4.7	29.5 ± 6.0 <sup>2</sup>	32.0 ± 5.9
Stature (in)	70.6 ± 2.8	70.5 ± 2.8	71.4 ± 2.4	70.7 ± 2.7
Weight (lb)	186.1 ± 21.8	186.3 ± 23.7	195.1 ± 22.8	187.8 ± 22.7
BMI (kg·m <sup>-2</sup> )	26.3 ± 2.5	26.4 ± 2.5	27.0 ± 2.8	26.4 ± 2.5
Years in Military	11.7 ± 5.7	13.8 ± 4.7	10.0 ± 5.1 <sup>3</sup>	12.0 ± 5.5
Years in SBU	4.5 ± 3.2	5.1 ± 2.7	4.7 ± 2.9	4.7 ± 3.0
<sup>1</sup> Values shown are means ± std. Dev.				
<sup>2</sup> Differs significantly ( <i>P</i> < 0.05) from SBU 12 and SBU 20 values.				
<sup>3</sup> Differs significantly ( <i>P</i> < 0.05) from SBU 20 value.				

The 154 respondents had 722 cumulative years of SBU exposure, and 100 respondents reported at least one injury. Most of the injuries were strains or sprains of muscles and joints, but fractures, dislocations, arthritis, and chronic pain were also reported [14]. Of particular note are the locations of the injuries, which are summarized in Table 3.

**Table 3. NHRC Survey Injury Locations [14]**

<b>Injury Location:</b>	<b># of Injuries at Location:</b>
Head	3
Neck/Upper Back	9
Shoulder	21
Elbow	2
Wrist	1
Hand	1
Trunk	2
Lower Back	50
Hip/Buttocks	6
Thigh	2
Knee	32
Leg	7
Ankle	10
Foot	3
<b>Total</b>	<b>149</b>

The majority of injuries occur in four locations: neck/shoulder, lower back, knee, and ankle regions. This data comes as no surprise, as these joints are particularly susceptible to normal shock events. The effects of shock on the human body will be discussed in Chapter 2.

Perhaps the most telling result of the survey is the correlation between injury and time spent in SBUs, which is shown in Figure 2.

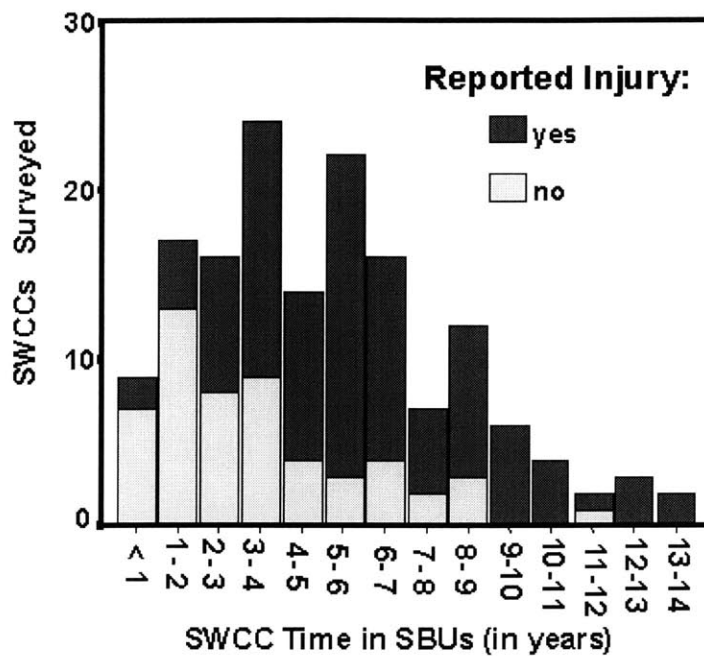


**Figure 2. Injuries vs. Time in SBUs [14]**

As seen in Figure 2, the rate of injury among SWCCs is directly proportional to time served in SBUs. In fact, by year ten, one hundred percent of SWCCs had an injury to report. In order to validate the survey results, a comparison of hospitalization rates of SWCCs to the Navy average was performed; Figure 3 summarizes the comparison.

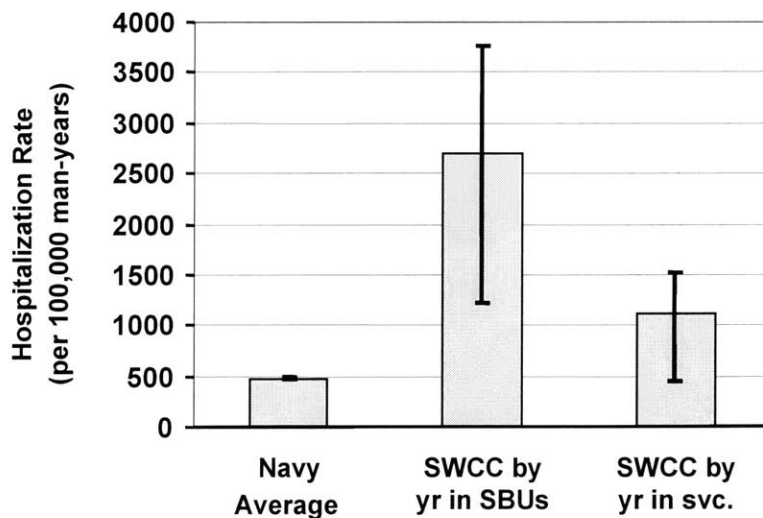


**Figure 3. Hospitalization Rates [14]**

When compared to the Navy as a whole, the hospitalization rates for SWCCs is significantly higher. Likewise, a SWCC attached to an SBU is more likely to be hospitalized than a SWCC not in an SBU. The study concluded that SBU personnel are at a greater than average risk for injury associated with SBU training and operations and that the closed-loop career path (i.e. SWCC rating) dictates rapid intervention [14].

Naval research and development efforts in the shock mitigation field accelerated as a result of the NHRC report. Rapid insertion of commercial technology is currently taking place in the form of deck padding and suspension seat mechanisms, but long-term solutions are required to maximize shock reduction potential. The Coastal Systems Station (CSS) of the Naval Surface Warfare Center (NSWC) coordinates shock mitigation research for the Office of Naval Research (ONR). This thesis project addresses a long-term hull geometry solution desired by CSS and is part of a total ship systems integration approach. By determining the effects of hull deadrise, cruise speed, and payload weight on vertical acceleration, future designers can more effectively design planing boats to meet NSW requirements and maximize mission effectiveness.

# Chapter 2

## The Mechanical Shock Environment

### 2.1 Hydrodynamics of the Hull-Sea Interface

High-speed planing boats were developed in the mid-1900s in order to achieve higher speeds than traditional displacement hulls. The benefits of the planing hull were indisputable, but the resulting hydrodynamics necessitated further research. This section summarizes planing hull resistance theory and briefly discusses the two major mechanisms of mechanical shock: wave slamming and vertical hull water entry. The coordinate reference system used in subsequent discussions is shown in Figure 4.

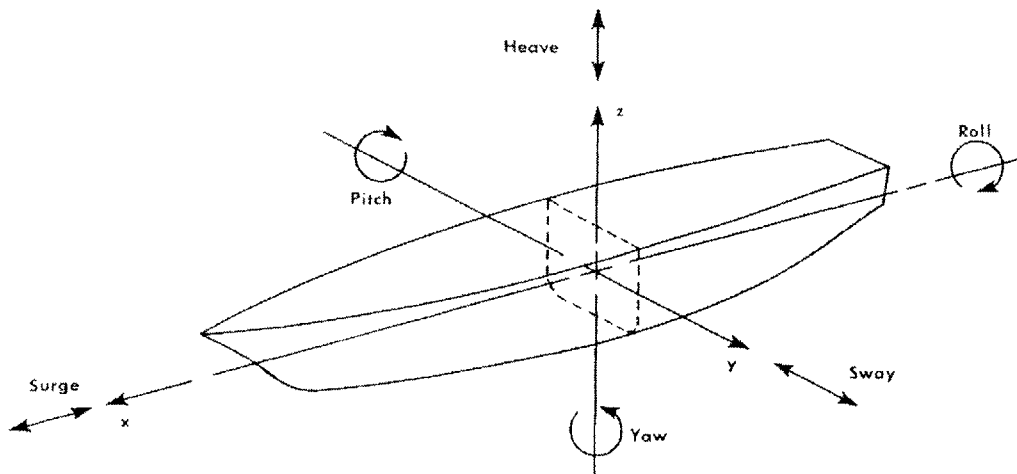


**Figure 4. Ship Motion Coordinate Reference [5]**

#### 2.1.1 Planing Hull Resistance Summary

The planing hull was developed in order to achieve high speeds. Speed is a function of total resistance ( $R_T$ ), which, for a displacement hull, is directly proportional to

the total resistance coefficient ( $C_T$ ), water density ( $\rho$ ), wetted surface area ( $S$ ), and the square of velocity ( $V$ ), as seen in Equation (1) [5].

$$R_T = \frac{1}{2} C_T \rho S V^2 \tag{1}$$

The only means by which a displacement hull can overcome large resistances to achieve high speeds is to increase shaft horsepower. By significantly reducing wetted surface area, the planing hull is able to achieve higher speeds than a monohull of comparable size. The development of lighter, more powerful engines in the 1930s facilitated the development of the planing hull [11].

While displacement hulls have longitudinal and transverse curvature, the planing hull has a transverse deadrise section and straight buttock lines to induce early flow separation. When a traditional displacement hull operates at high speeds, the negative dynamic pressure induced on the convex hull surfaces causes a large trim by the stern, increasing resistance. The planing hull is designed to develop positive dynamic pressure, so the displacement decreases with increasing speed [11]. Figure 5 shows the relationship between lift fraction and speed for a typical planing hull.

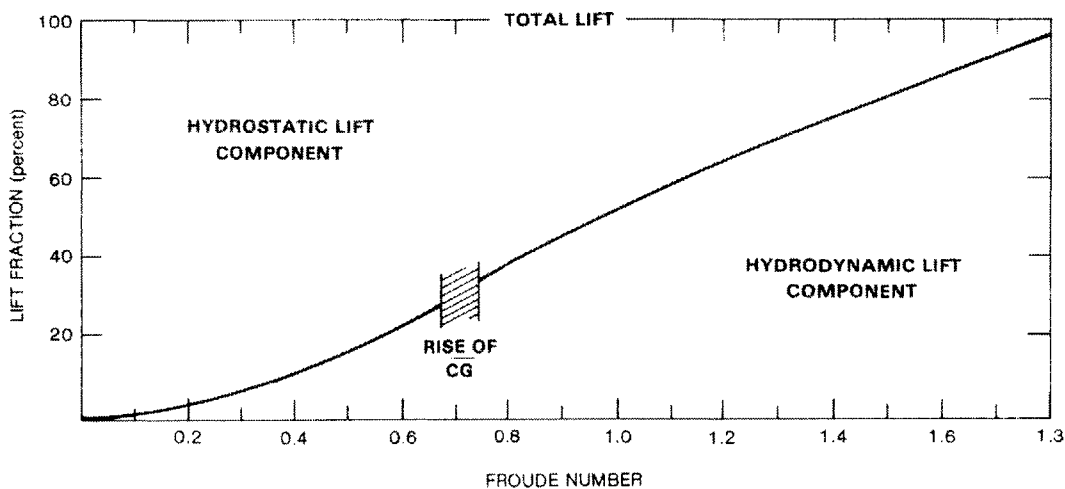


**Figure 5. Lift Fraction vs. Froude Number [11]**

The nondimensional Froude number,  $Fn$ , is given by Equation (2), where  $g$  is the acceleration due to gravity and  $L$  is the length of the vessel.

$$Fn = \frac{V}{\sqrt{gL}} \quad (2)$$

The hydrodynamics of the planing hull result in a reduction of wetted surface area of up to 60% and therefore enable much higher speeds [11].

[16] and [17] summarize the development of the planing hull and develop formulas for lift and drag forces on a planing hull. [7] used [16] to develop a method to predict the resistance of a planing hull. The free body diagram of a planing hull is shown in Figure 6 [16]. In this diagram,  $W$  is the weight of the boat,  $T$  is the propeller thrust,  $D_f$  is the frictional drag,  $N$  is the component of resistance normal to the bottom, and  $\tau$  is the trim angle of planing area.

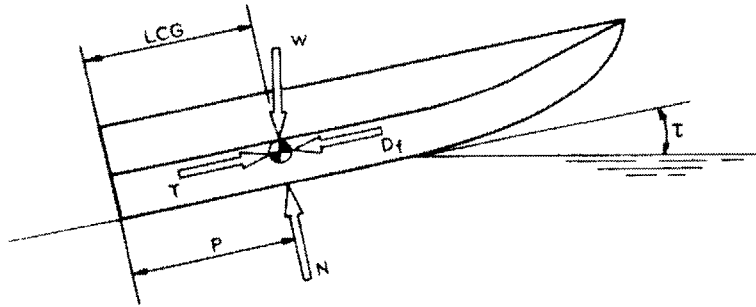


**Figure 6. Free Body Diagram of a Planing Hull [16]**

The total resistance,  $R_T$ , of the planing hull can be predicted by Equation (3).

$$R_T = W \tan \tau + \frac{\frac{1}{2} \rho V^2 \lambda b^2 C_{FO}}{\cos \tau \cos \beta} \quad (3)$$

In Equation (3),  $\lambda$  is the mean wetted-length to beam ratio,  $b$  is the beam of planing area,  $C_{FO}$  is the ITTC friction coefficient, and  $\beta$  is the mid-chine deadrise [11]. The goal of this study is to vary  $\beta$  and analyze the subsequent vertical acceleration and craft resistance. As will be seen in Chapter 3, a change in  $\beta$  will cause the vessel to operate at a new  $\tau$ , both of which affect resistance and vertical acceleration.



### **2.1.2 Wave Slamming**

Wave slamming is a term used to describe the emergence of the bow of the ship and subsequent impact of the ship's bottom on the surface of a wave. Slamming can cause structural damage and induce transient vibratory stresses throughout the hull. For planing craft operating at high speeds, slamming forces are due to the combined effects of the vertical relative motion between the ship and the sea and the forward motion of the boat through the waves [11]. Historically, slamming forces have been modeled primarily to determine ship structural requirements and not effects on personnel. The object of this thesis is to create a hull to minimize heave accelerations due to slamming in order to reduce the magnitude of the shock pulse entering the hull.

Slamming causes high impact pressures under the bow of the ship. Prediction of these impact pressures is complex and inexact, but some theories have been proven accurate by various drop-tests. [20], for example, developed expanding plate theory in 1929 in order to predict slamming behavior for seaplanes. Determination of slamming forces on vessels is primarily an empirical endeavor. Qualitatively speaking, the following factors influence slamming: relative vertical velocity at the bow entry point, sectional shape, angle between the keel and wave slope at entry, area of impact, and duration of impact [11].

### **2.1.3 Vertical Hull Water Entry**

Vertical water hull entry occurs when a HSPB fully leaves the surface of the water and then re-enters the water at some angle relative to the sea. The dynamics of this hull-sea interaction are not well known. The theory of vertical hull water entry is more complex than wave slamming due to the unknown height the boat reaches and subsequent re-entry angle. These two parameters largely determine the magnitude and duration of the shock pulse that enters the hull. [22] analyzed vertical hull water entry and empirically validated their prediction models. [12] developed the Water Entry Dynamics and Injury Model (WEDIM) to model hull entry in order to predict shock forces on NSW HSPBs. Research on the forces due to vertical hull water entry is ongoing. Chapter 3 will show how changes in hull deadrise affect the forces induced by vertical hull water entry and slamming.

## 2.2 Effects of Mechanical Shock

Mechanical vibration has been studied for hundreds of years, normally for the purposes of structural design. Mechanical vibration concerns oscillatory motion over a period of time, and is normally described by frequency and amplitude. Vibration can be free or forced, deterministic or random, and is normally periodic. Shock is generally defined as an aspect of vibration where the excitation is nonperiodic and occurs suddenly [19]. A typical shock event for a HSPB is shown in Figure 7.

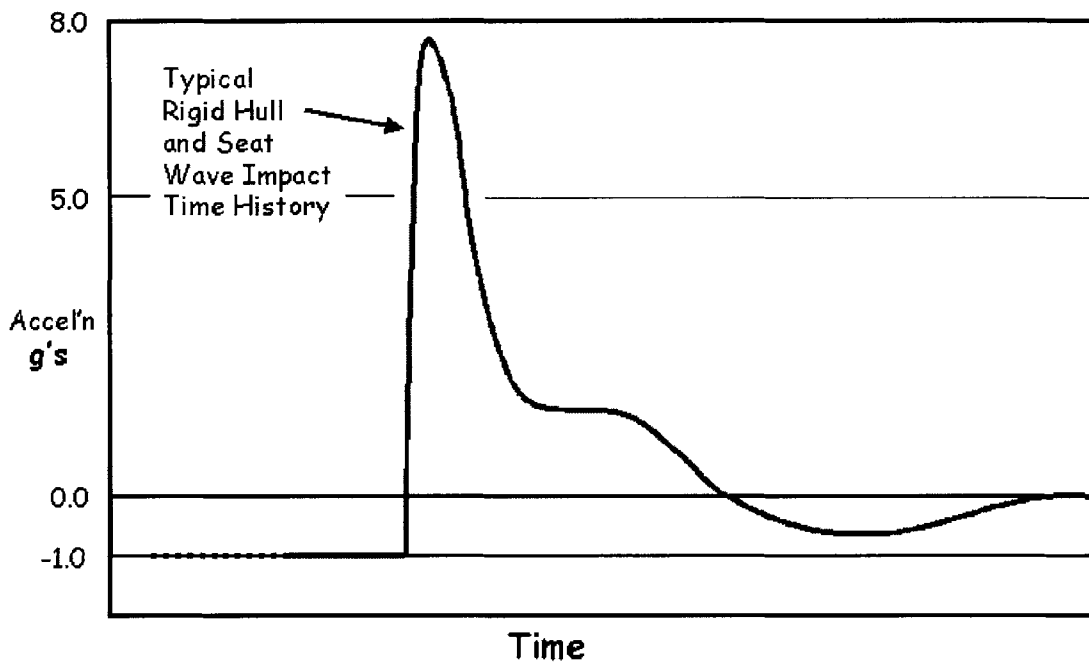


**Figure 7. Typical HSPB Shock Event [13]**

The waveform shown in Figure 7 displays the peak acceleration, which is the greatest positive or negative sample point that encountered for the shock event. Generally, the duration of the shock event is 30-75 msec, depending on boat speed, sea state, etc. To put these values into perspective, Table 4 shows the approximate duration and magnitude of some common short-term acceleration loads.

**Table 4. Summary of Short-Duration Acceleration Loads [19]**

Type of Operation	Acceleration (g)	Duration (sec)
Elevator		
Average (fast service)	0.1-0.2	1-5
Emergency Deceleration	2.5	-
Automobile		
Comfortable Stop	0.25	5-8
Max. Obtainable	0.7	3
Crash	20-100	<0.1
Aircraft		
Ordinary Take-off	0.5	>10
Catapult Take-off	2.5-6	1.5
Crash Landing	20-100	-
Seat Ejection	10-15	0.25
Human (head)		
Adult falling from 6 ft onto hard surface	250	0.007
Voluntarily tolerated impact with head protection	18-23	0.02

The study of the effects of vibration on humans is a relatively new field that has developed largely as a result of numerous advances in human transportation. [19] presents a thorough description of research into the effects of shock and vibration on humans. Only a short description of the effects of shock on humans will be discussed in this section.

As the establishment of limits for human tolerance to mechanical vibration requires potentially hazardous experimentation, humans are not used as test subjects. Animals, dummies, or cadavers are frequently used to determine suitable vibration limits for humans [19]. The physiological differences in these test subjects must be accounted for during the testing. Though such testing is clearly not exact, it is perhaps the most accurate simulation currently possible. Significant data has been collected on human body response testing over the years. Figure 8, for example, shows the effect of fatigue on bone and cartilage failure.

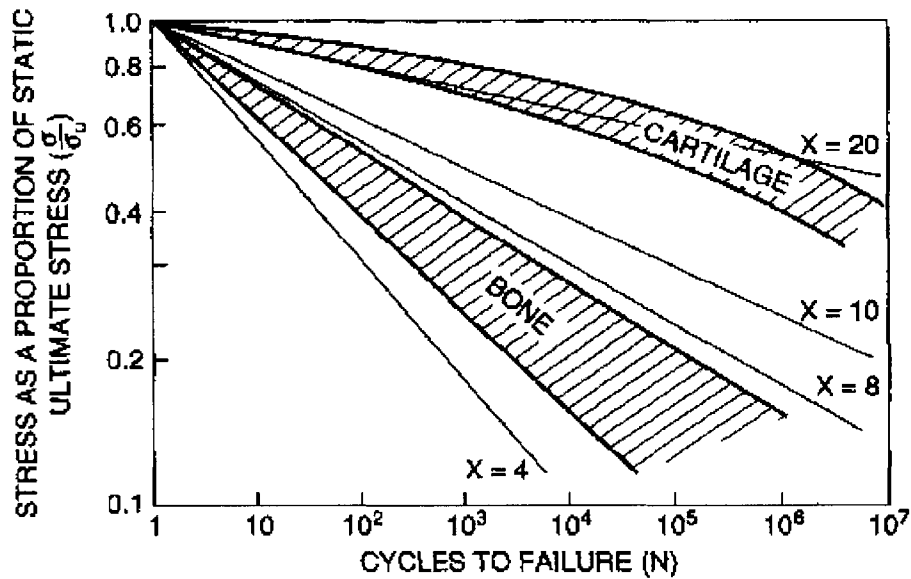


**Figure 8. Effect of Fatigue on Bone and Cartilage Failure [19]**

The straight lines in Figure 8 represent the function

$$N = \left(\frac{\sigma}{\sigma_U}\right)^{-x}, \quad (4)$$

where the value of the index  $x$  is indicated in the figure. As the body is subjected to an increasing number of stress events, the stress required for failure is reduced for both bone and cartilage [19]. This relationship is true for *in vitro* samples and does not account for the regenerative effects of living bone tissue with regard to stress.

The concept of the Dynamic Response Index (DRI) was created in the 1970s to quantify the potential for spinal injury due to large vertical accelerations. This DRI research was further developed by the Air Standardization Coordinating Committee in order to evaluate exposure to repeated shocks to the body. Figure 9 shows the relationship between shock magnitude and number of shock events.

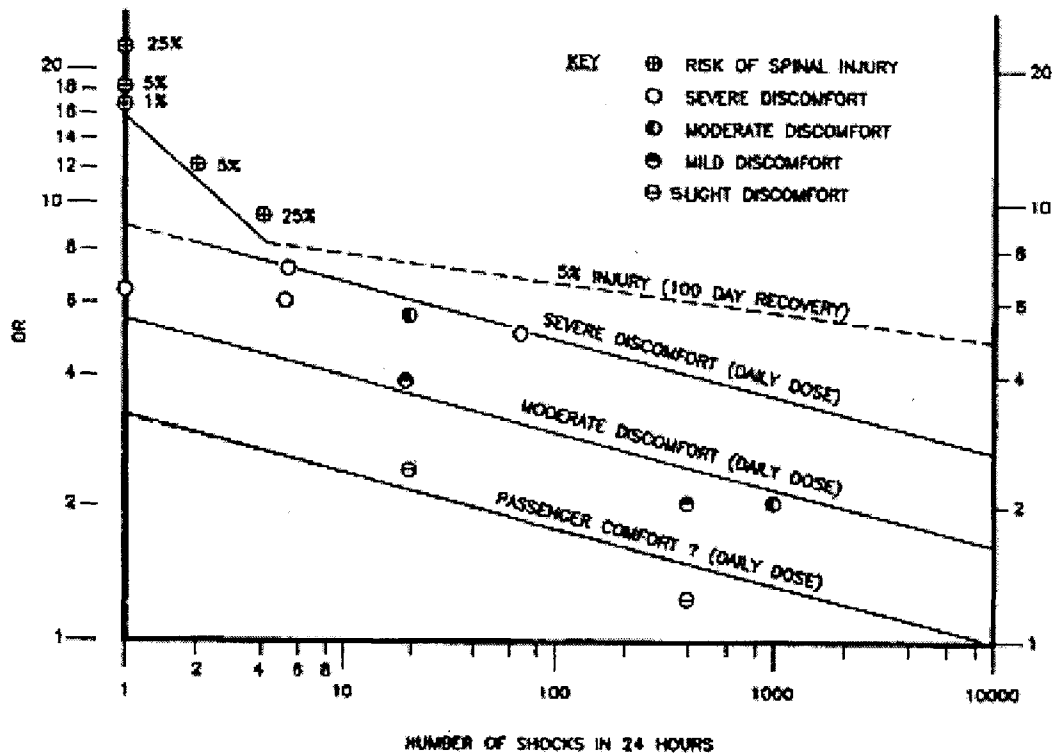


Figure 9. Injury and Discomfort Limits for Repeated Shocks [19]

In this case, DR is the maximum static acceleration (above normal gravity). The circles represent exposures to which the risk of injury has been documented [19].

In summary, there are documented risks associated with exposure to mechanical shock. Although limits for human exposure to shock have been developed, there is much controversy surrounding the accuracy of these limits and the methodology used to determine such limits. Numerous government and civilian organizations continue to research these concepts in order to develop reliable human injury models. With regard to boat design, the designer must find some way to produce a design that does not result in excessive shock. Until specific limitations are developed for HSPB operators, designers will adhere to the theory that the smaller the magnitude and duration of the shock pulse, the better. While this may indeed be a true statement, it does not allow the designer much flexibility. The next section briefly summarizes the concepts being explored pertaining to shock mitigation of HSPBs.

### 2.3 Shock Mitigation Concepts

There has been much study in the field of mechanical shock reduction. The automotive industry, for example, has nearly perfected the suspension system, which is used to create a smooth ride for passengers. Although a comparison of automotive and HSPB operations seems obtuse, there are some interesting similarities between the two systems. An automotive engineer must consider operating environment, vehicle size, operator control, and cost, among other things, when designing a system to minimize shock transmitted to passengers. Creating a successful system for a HSPB operating in rough seas is a similar process. The causes of shock are known, but there are numerous different mitigation systems with varying performance characteristics. The methods of mitigating shock are generally classified as design or operational concepts. Operational concepts, such as training and physical conditioning, are well known and currently in use. This section summarizes the various design methods used to mitigate shock, which fall into the three categories shown in Figure 10.

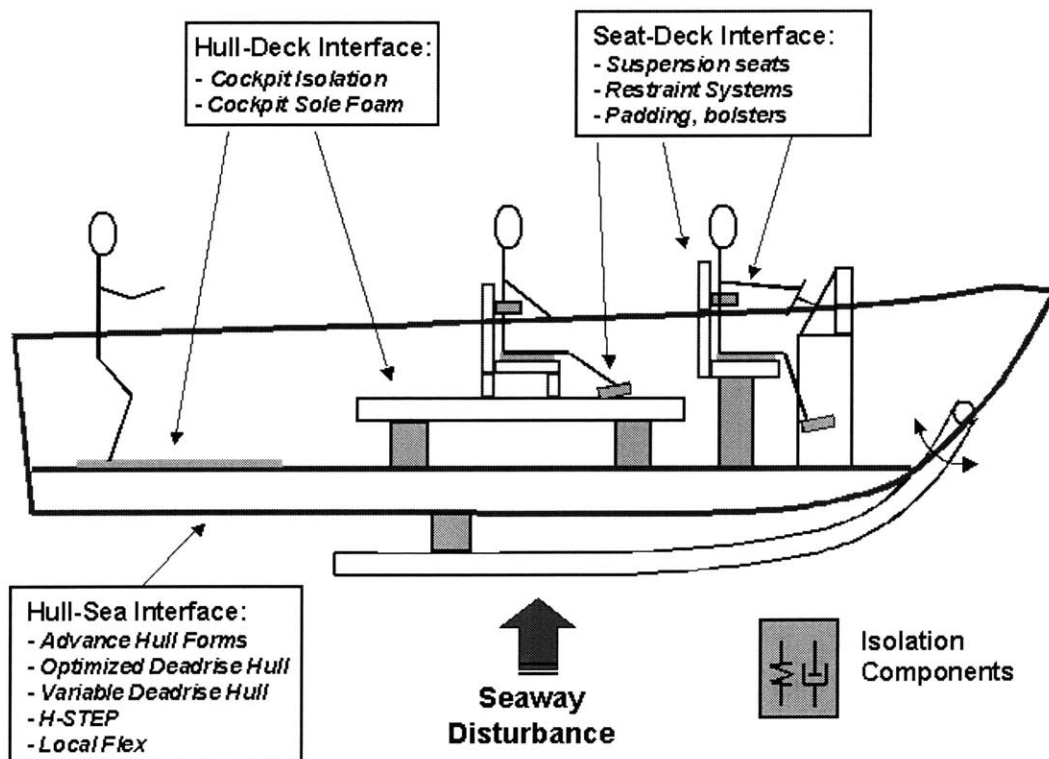


Figure 10. Design Methods for Shock Mitigation [13]

### 2.3.1 Hull-Sea Interface

The logical way to reduce the effects of mechanical shock on a boat and its occupants is to reduce the magnitude and duration of the shock event. The effects of weaker shock events may then be further reduced during transmission by using deck-hull or seat-deck mitigation systems. Therefore, some form of hull-sea mitigation is required to maximize reduction in shock. However, this is by far the most difficult, time-consuming, and expensive solution. Previous research has demonstrated the reduction in wave slamming forces realized in using a v-shaped hull. Current research in the hull-sea interface area focuses on modification of existing hulls and development of new hull geometries. The goal of this research is to reduce the vertical acceleration of the boat upon impact with the sea, which reduces the shock force transmitted to the hull.

### Hull Geometry Solutions

Research and development of advanced hull forms is a continuous process, though not necessarily for the purposes of shock mitigation. Only recently have alternative hull forms been considered for NSW boat designs. Due to the high speed requirements of NSW watercraft, displacement hulls are poor candidates, as hull resistance is much too high. Figure 11 shows the broad range of high-speed hull forms.

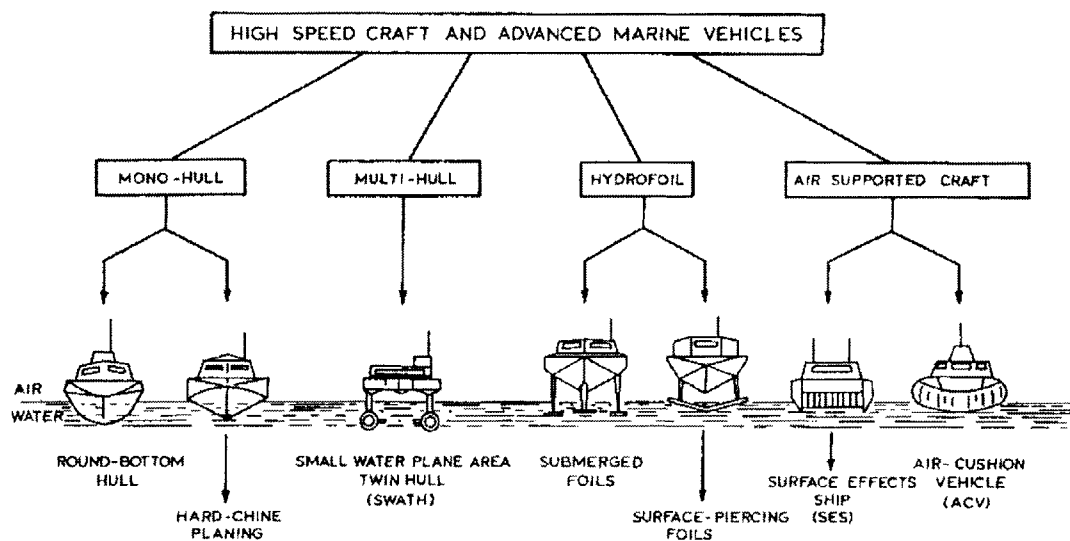


Figure 11. High Speed Hull Forms [11]

Hydrofoils and air cushion vessels (the PHM-1 Pegasus class ships and Landing Craft, Air Cushion transporters, for example) have been used successfully in the past to achieve high speeds and moderately smooth rides. However, current designs are range- and payload-limited, making them inadequate platforms for SEALs. Multi-hull craft such as SWATHs and catamarans may prove useful but require further development to meet NSW requirements. The most promising hull form currently under consideration is the Very Slender Vessel (VSV), which is shown in Figure 12.



**Figure 12. Very Slender Vessel [4]**

The VSV, which was developed in conjunction with Defense Advanced Research Projects Agency (DARPA) and the Office of the Secretary of Defense (OSD) Technical Support Working Group (TSWG), was designed as a wave-piercing hull [4]. As a result, the wave slamming effects are reduced, and the vertical hull water entry effects are entirely eliminated, since the boat remains in the water. Hull forms such as the VSV, which is currently being tested, may prove to be viable platforms in the future.

Though advanced hull form research is promising, planing hulls are still the platform of choice for high-speed craft. CSS directs several research efforts in coordination with government and institutional organizations. In the late 1990s, CSS collaborated with the University of Michigan to create the ODH concept. The existing



ZARN software code used for planing boats was modified to handle non-constant longitudinal deadrise, later culminating in the creation of the POWERSEA software code. A family of four simple deadrise variations was developed in order to predict the corresponding resistance and accelerations of the variants. The study concluded that slight changes in deadrise can significantly reduce bow and center of gravity (CG) accelerations with no increase in hull resistance; a three degree increase in forebody deadrise decreased vertical acceleration by twelve percent [13]. This pilot study is the extent of ODH research to date. In 1999, at-sea testing validated the POWERSEA predictions. The goal of this thesis was to investigate the ODH concept further with the use of POWERSEA.

### **Hull Modification Solutions**

The two major hull modification efforts performed in the late 1990s involved the Hinged-Step for Enhanced Performance (H-STEP) and LocalFlex technologies. CSS developed the H-STEP shock reduction concept and performed at-sea testing of a scale model in 1996. The H-STEP method utilizes a rigid, moving outer hull section that is hinged near the bow in conjunction with an air shock system placed between the inner (boat) and outer hulls. Figure 13 depicts the H-STEP system.

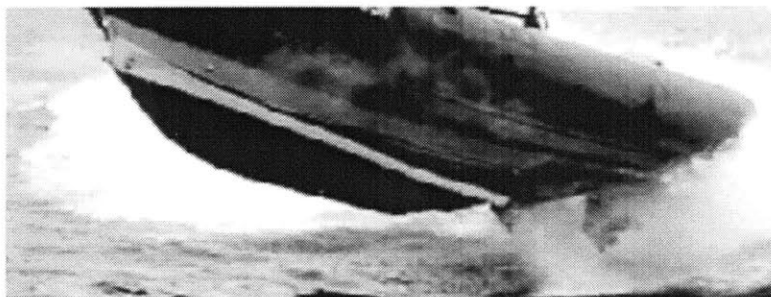


**Figure 13. H-STEP [13]**

The scale model testing results revealed an average of thirty-five percent reduction in vertical acceleration and an average of eight percent increase in speed. However, the tests also showed some limitation of the current H-STEP design, as there were adverse

effects on weight and maneuvering [13]. Although no additional research was performed, H-STEP is a promising technology.

LocalFlex is a system created by Vorus at the University of New Orleans. Like H-STEP, it is an external hull attachment that can be configured for existing hull shapes. LocalFlex, shown in Figure 14, consists of aluminum plates hinged at the keel, supported by air bags at the chines.

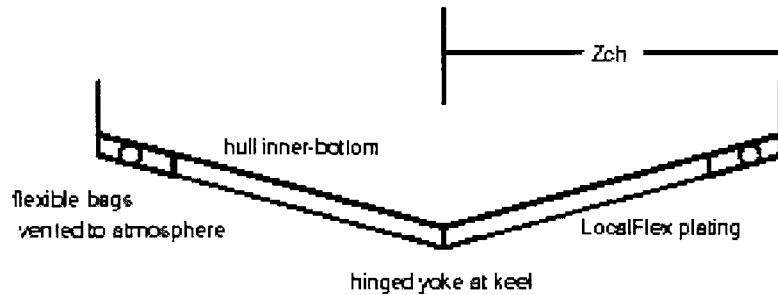


**Figure 14. LocalFlex [14]**

A prototype of this system was developed and tested in 2000. Testing revealed that LocalFlex is an effective shock reduction mechanism, but it lacks the ability to recover its shape between shock events [14].

### **2.3.2 Deck-Hull Interface**

The deck-hull interface offers some of the easiest and most inexpensive methods of shock reduction. The most common item used to mitigate shock at this location is rubber or foam padding, which can be used as a simple deck covering. As expected, the ability of these components to significantly reduce shock is limited, since their effectiveness is limited by the amount of displacement available. Due to the limited available space on HSPBs, such padding offers little benefit. Advancements in cushioning technologies have produced higher quality foam, which is generally used to absorb engine and propeller vibrations. Although padding offers small benefit, it does provide some absorption and can be combined with other systems to increase overall effectiveness.

The most promising method of reducing shock at the deck-hull interface is cockpit isolation. In this case, the cockpit of the vessel is suspended, so it is physically

isolated from the deck. For many boats, the space between the deck and the hull offers the most available displacement room. [10] used the single degree of freedom model in [9] to evaluate a passive shock isolation system having approximately twelve inches of available displacement. Preliminary results showed a sixty percent reduction in shock pulse magnitude for a 50-msec pulse and thirty-five percent reduction for a 100-msec pulse [10]. Cockpit isolation is a long-term solution that could be incorporated in a combined shock mitigation system on future HSPBs.

### **2.3.3 Seat-Deck Interface**

Perhaps the most feasible short-term solution to the shock mitigation problem is located at the seat-deck interface. Commercially developed suspension seats are currently being evaluated and tested to determine their effectiveness. The MkV SOC has a STIDD 800v4 seat, which has no suspension system. In January 2002, a maritime operational test and evaluation of three candidate suspension seats was conducted by [3]. The most effective suspension seat proved to be the STIDD 800v5, which is an existing MkV SOC seat with a load adjusting spring and a shock absorber base with a dampening speed control mechanism. This seat requires few modifications to the existing boats and represents the best bolt-on solution currently available [3].

Other shock mitigation systems found at the seat-deck interface include restraint systems and padding. Current MkV SOC seats include padding and restraints, but these systems were designed for comfort and safety, not necessarily to mitigate shock. CSS continues to investigate new padding and restraint systems.

# Chapter 3

## Optimal Deadrise Hull Analysis

### 3.1 Design Tool Description

The POWERSEA Time-Domain Planing Hull Simulation software was used to create an ODH. POWERSEA was created by Ship Motion Associates and is largely based on theory developed by Zarnick in 1978. The material in this section is discussed in great detail in [1]. Zarnick developed a low-aspect ratio strip theory to predict vertical-plane motions of planing craft. Zarnick assumed that wavelengths are large with respect to craft length and that wave slopes are small. He modeled planing craft as a series of two-dimensional impacting wedges, as shown in Figure 15.

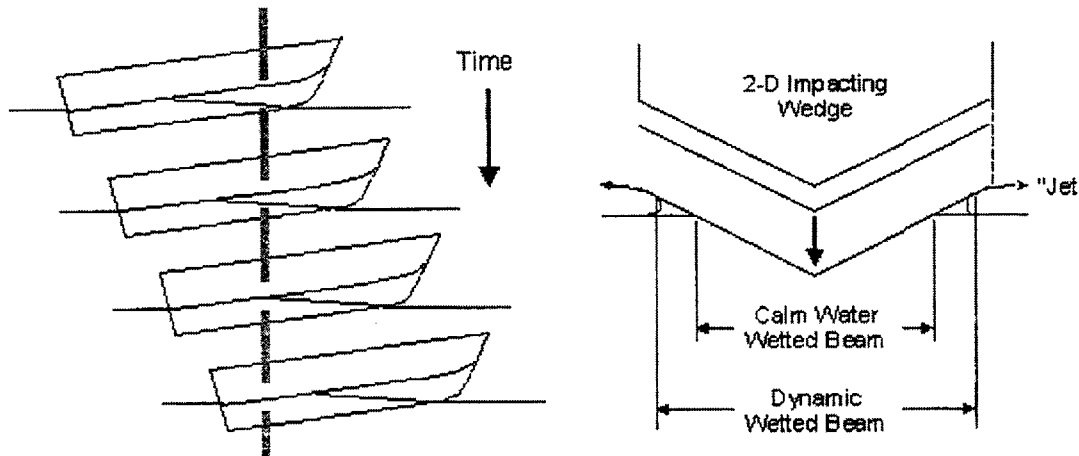


Figure 15. Impacting Wedges [1]

Zarnick derived the normal hydrodynamic force per unit length,  $f$ , as the sum of a Newtonian force term and a cross-flow force term, respectively:

$$f = -\left\{ \frac{D}{Dt} (m_a V) + C_{D,c} \rho b V^2 \right\} \quad (5)$$

$$\text{where } \frac{D}{Dt}(m_a V) = m_a \dot{V} + \dot{m}_a V - \frac{\partial}{\partial t}(m_a V) \frac{d\xi}{dt}. \quad (6)$$

In Equation (5),  $m_a$  is the sectional added mass,  $V$  is the velocity of the boat in the vertical direction (refer to Figure 4),  $C_{D,c}$  is a cross-flow drag coefficient,  $\rho$  is water density, and  $b$  is the sectional half-beam. In Equation (6),  $\xi$  is the longitudinal boat coordinate measured from the boat's longitudinal center of gravity. Sectional added mass is modeled as if it were an impacting wedge:

$$m_a = k_a \frac{\pi}{2} \rho b^2 \quad (7)$$

$$\dot{m}_a = k_a \pi \rho b \dot{b} \quad (8)$$

$$k_a = \frac{\pi^2}{4} \{1 - 0.4 \frac{\beta}{90} (1 - KAR)\} \quad (9)$$

where  $k_a$  is an added mass coefficient that is deadrise-dependent,  $\beta$  is the deadrise of the prismatic hull, and  $KAR$  is an added mass correction factor [1].

A summary of the forces acting on the planing boat is:

$$F_N = \int \{m_a \dot{V} + \dot{m}_a V - U \frac{\partial m_a}{\partial \xi} + C_{D,c} \rho V b^2\} d\xi \quad (10)$$

$$F_Z = -F_N \cos \theta - \int \rho g C_{BF} a d\xi \quad (11)$$

$$F_X = -F_N \sin \theta \quad (12)$$

$$F_\theta = \int \{m_a \dot{V} + \dot{m}_a V - U \frac{\partial m_a}{\partial \xi} + C_{D,c} \rho V b^2 - \rho g C_{BM} a \cos \theta\} \xi d\xi \quad (13)$$

In Equations (10) through (13),  $F_N$  is the force normal to the boat hull,  $F_Z$  is the vertical force,  $F_X$  is the horizontal force,  $F_\theta$  is the moment in the pitch direction,  $U$  is the velocity of the boat in the x-direction,  $C_{BM}$  is the buoyancy moment coefficient,  $C_{BF}$  is the buoyancy force coefficient,  $a$  is the sectional area, and  $\theta$  is the pitch angle [1].

The resulting equations of motion are:

$$M \ddot{x}_{CG} = T_X - F_N \sin \theta - F_D \cos \theta \quad (14)$$

$$M \ddot{z}_{CG} = T_Z - F_N \cos \theta - F_B + F_D \sin \theta + W \quad (15)$$

$$I \ddot{\theta} = T x_p + F_N x_C - F_B x_B - F_D x_D. \quad (16)$$

In Equations (14) through (16),  $M$  is the mass of the boat,  $x_{CG}$  is the x-direction center of gravity,  $z_{CG}$  is the z-direction center of gravity,  $T$  is thrust force,  $F_D$  is total drag force in the x-direction,  $F_B$  is the buoyancy force,  $W$  is the weight of the boat,  $I$  is the pitch moment of inertia,  $x_P$  is the distance from CG to the thrust vector,  $x_C$  is the distance from CG to the center of the normal force,  $x_B$  is the distance from CG to the center of buoyancy, and  $x_D$  is the distance from CG to the center of action of the drag force. The POWERSEA algorithms numerically solve the equations of motion for specified geometry and initial conditions [1].

### 3.2 Design Methodology

A design model of the MkV SOC was created using known dimensions of the boat. Unfortunately, the specific boat geometry was unavailable for this thesis due to proprietary reasons. As a result, the model was developed based on available data and dimensions were scaled appropriately by visual inspection. Table 5 summarizes the principal characteristics of the MkV SOC model, and Figure 16 shows the midship section of the model.

**Table 5. MkV SOC Model Principal Characteristics**

Length Overall	82 ft	Forebody Deadrise	35°
Maximum Beam	17.5 ft	Mid-chine Deadrise	29°
Depth (Keel to Shear)	7.75 ft	LCG	30 ft aft FP
Maximum Chine Depth	4.75 ft	VCG	2.5 ft ABL
Displacement	119000 lbs	Radius of Gyration	20 ft

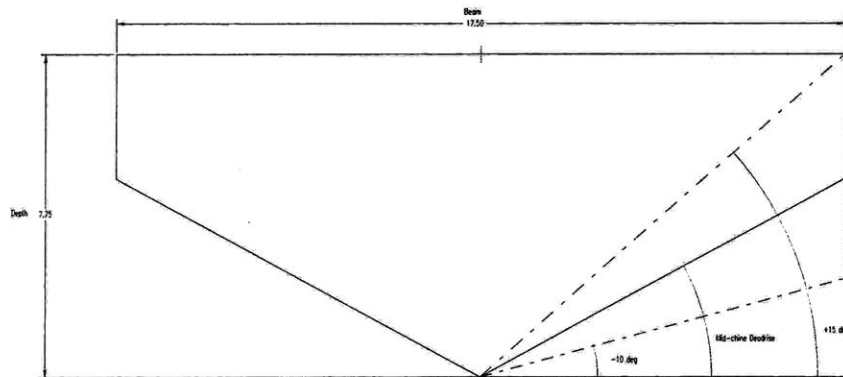


**Figure 16. MkV SOC Design Model**

The overall dimensions of the MkV SOC are limited by transportation requirements. A MkV SOC detachment, which includes two boats, fits inside a US Air Force C-5 Galaxy cargo aircraft. Therefore, all models created for this analysis have the same overall length, beam, and depth as the MkV SOC in order to ensure space limits are not exceeded. Despite these fixed parameters, the deadrise can be varied by changing the vertical location of the chine. A family of twenty-six hulls with deadrise values ranging from fifteen to forty degrees was created and analyzed to determine the effects of deadrise on heave acceleration. In general, the afterbody deadrise, henceforth referred to as mid-chine deadrise, is nearly constant from amidships to the stern, and the forebody deadrise is slightly higher. The maximum deadrise of forty degrees is illogical, as the chine and shear lines are identical, resulting in a simple v-shape that lacks interior volume for arrangements. However, in order to generate data for a larger range of geometries, such high values of deadrise were used in the analysis.

Both calm water and rough water sea conditions were applied to each model. The calm water simulation provided a running trim angle and other hydrodynamic parameters required for the rough water simulation. Additionally, the calm water analysis predicted resistance and required power for a given speed. A rough water simulation was then performed to determine heave acceleration. Table 6 summarizes the inputs provided for the rough water simulation.

**Table 6. Input for Rough Water Simulation**

<b>Parameter</b>	<b>Value</b>
Boat Speed	35 kts
Wave Conditions	ITTC Peak Frequency Spectrum
Significant Wave Height	3.1 ft
Peak Period	5.5 sec
Water Depth	Deep Water
Wave Direction	Head Seas
Location	Coxswain

The ITTC Peak Frequency Spectrum was chosen to simulate random seas. The boat speed, significant wave height, peak period, water depth, and wave direction were chosen to duplicate sea conditions that existed for at-sea testing of the Mk V SOC.

The MkV SOC was tested on multiple occasions by the Naval Surface Warfare Center Combat Craft Division in the late 1990s. Acceleration data was recorded at four different boat locations and under various sea conditions. In order to validate the POWERSEA predictions, rough water simulations were performed in the sea conditions that existed during the at-sea testing. The craft was tested at a nominal displacement that represented the typical half-load condition existing on the return leg of a mission. The sea state was 2-3, with a significant wave height ( $H^{1/3}$ ) of 3.1 ft. The specific test used for comparison is the case in which accelerations were measured at the Coxswain location for operation at 35 kts in head seas. The actual test results [8] are restricted and therefore not printable in this report.

The at-sea testing measured heave, surge, and sway peak and RMS accelerations and the duration of each pulse. POWERSEA does not calculate sway acceleration, and for a constant surge velocity, surge acceleration is zero. Therefore, the only POWERSEA calculation of interest is heave acceleration, which is due to the heaving and pitching motions of the boat. In both at-sea and simulation scenarios, heave acceleration dominates craft motion and therefore controls the mechanical shock event.

The simulations proved to be relatively accurate when compared to the at-sea testing values. However, there are several reasons for the small discrepancies between the simulated and actual values:

- The actual offsets of the MK V SOC were unavailable due to proprietary reasons, so the simulation model has slight differences in geometry.
- The simulation used a random sea generation based on an ITTC spectrum with  $H^{1/3}$  of 3.1 ft and peak frequency of 5.5 sec, which matches but does not duplicate the sea conditions during the tests.
- The at-sea testing accelerometers had threshold settings in order to trigger the device and avoid recording negligible acceleration values.

Based on these simulations, the software is relatively accurate in its predictions of accelerations and is therefore a valid analysis tool.



### 3.3 Design Results

In order to determine the effects of deadrise on vertical acceleration, all twenty-six hulls were simulated in the same sea conditions described in Table 6. Calm water simulations were performed to evaluate the resistance of the hull, and rough water simulations were performed to determine heave acceleration at the coxswain location. All POWERSEA data collected during the ODH simulations is included in Appendix A. Table 7 summarizes the resistance and heave accelerations at the coxswain location for each model, and Figure 17 displays the percent change of resistance and heave accelerations from baseline.

**Table 7. Resistance and Coxswain Heave Acceleration Results**

<b>Forebody Deadrise (deg)</b>	<b>Mid-chine Deadrise (deg)</b>	<b>Resistance (hp required for 35 knots)</b>	<b>Average Heave Acceleration (g)</b>	<b>1/3 Highest Heave Acceleration (g)</b>
19.5	15	1307.3	0.33	2.35
20.8	16	1332.1	0.32	1.83
21.7	17	1355.9	0.33	2.10
22.2	18	1390.0	0.28	2.02
23.1	19	1410.6	0.33	2.03
24.3	20	1439.5	0.31	2.26
26	21	1453.2	0.30	1.77
28.4	22	1450.5	0.29	1.54
28.8	23	1485.9	0.30	1.57
31.1	24	1513.8	0.28	1.26
33.1	25	1522.8	0.27	1.28
33.5	26	1560.7	0.27	1.15
33.9	27	1594.3	0.28	0.97
34.1	28	1632.1	0.27	1.16
34.5	29	1661.3	0.26	1.01
34.8	30	1689.6	0.24	0.89
35.2	31	1714.3	0.22	0.81
35.6	32	1646.3	0.22	0.83
37.5	33	1601.3	0.24	0.92
38	34	1616.8	0.23	0.92
39	35	1614.1	0.21	0.78
40	36	1618.8	0.21	0.83
41	37	1620.4	0.21	0.72
42	38	1610.0	0.20	0.71
43	39	1599.9	0.20	0.80
44	40	1597.5	0.18	0.72

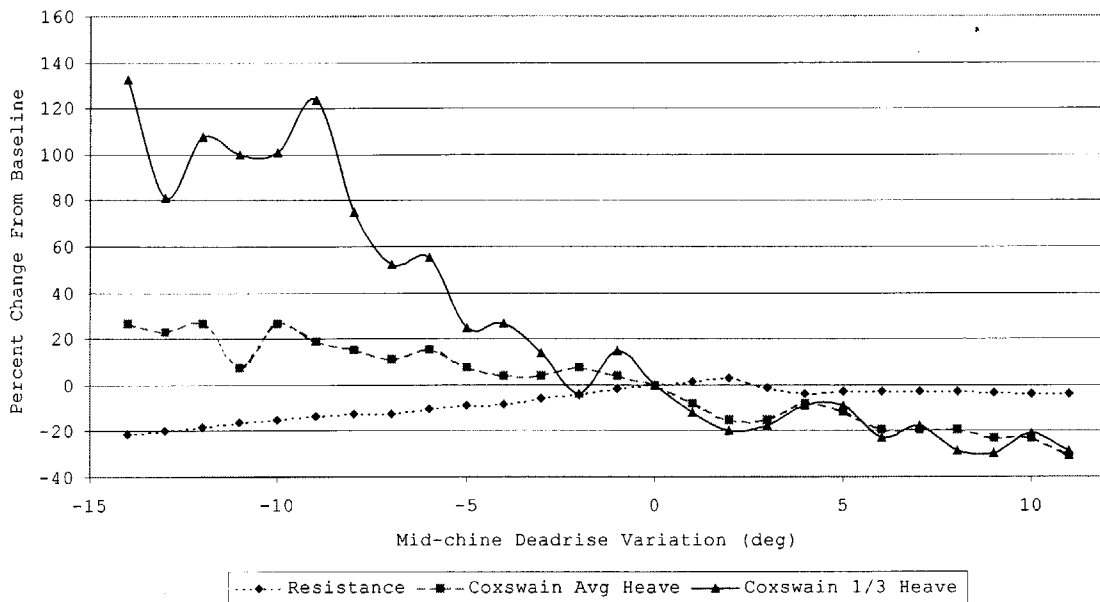


**Figure 17. Percent Change From Baseline**

The 1/3 highest heave acceleration represents the average of the 1/3 highest values of the heave acceleration at the coxswain location. Although there is some data scatter due to the random seas generated by the ITTC wave energy spectrum, the relationship between deadrise and heave acceleration is clear. The trends in Figure 17 show that higher values of deadrise can significantly reduce vertical acceleration of the boat while maintaining current speed capabilities. As a result of these lower accelerations, the mechanical shock transmitted to the crew and passengers would be greatly diminished.

The results of this Optimal Deadrise Hull analysis show similar trends to the results obtained in the relatively limited computations performed at University of Michigan (UM) using the modified ZARN coding. As POWERSEA was later developed from this code and refined to match the results of planing boat model testing, it is noteworthy that the analyses provide similar results. In order to establish a broader trend, twenty-six hulls were analyzed, whereas the previous analysis at UM only considered four hulls. The general results from both analyses show that as deadrise is increased, resistance gradually increases but vertical acceleration decreases at a faster rate. The ODH analysis shows asymptotic behavior, as both resistance and vertical acceleration level out at higher values of deadrise.

Realistically, the maximum deadrise values are undesirable for the current MkV SOC geometry. The most feasible solution for the specific boat geometry is to increase deadrise by about six degrees, which provides a twenty percent reduction in average heave acceleration and twenty-three percent reduction in 1/3 highest heave acceleration. For this case, resistance improved by approximately three percent so no loss in speed was realized. In order to fully realize the possibilities, different boat geometries must be tested over a range of displacements. The geometry and displacement of the MkV SOC were fixed for the purposes of this project in order to ensure the boat remained transportable via current methods.

# Chapter 4

## Design Space Study

### 4.1 Response Surface Methods

During any design process, many factors must be considered. For the MkV SOC, transportation was a major factor; the ability to fit two boats into a USAF C-5 Galaxy aircraft was a strict geometrical limitation. Other factors, such as payload capacity, number of passengers, and speed were important but perhaps to a lesser degree. For future designs, mechanical shock will undoubtedly be a design factor. Its importance relative to other design criteria may or may not be determined before design work begins. This section demonstrates a top-level design process called Response Surface Methods (RSM), which creates a design space using a design of experiments (DOE), allowing designers to compare feasible designs as part of a multiple criteria decision making process.

This section outlines the basic concepts of RSM required to understand the design space studies presented in this report. There are several references available for a more detailed understanding of RSM. [6] provides an overview and application of RSM to submarine concept design and [18] is an excellent text on the underlying concepts behind RSM .

The following terminology is used in the RSM discussion:

- Factors: The input variables or design parameters, represented by  $x_i$ .
- Levels: The different settings for each factor. For a two-level factor, the low-level is represented by (-1) and the high-level as (+1). For a three-level factor, the intermediate level is represented by (0).
- Response: The output of interest, represented by the letter  $y$ .

- Interactions(s): Refer to dependencies between a factor's effect on the response and levels of another factor. The interaction of  $x_1$  and  $x_2$  is represented as  $x_1x_2$  [6].

RSM is a statistical technique used to study the significance of the shift in mean value of a response due to a shift in factor levels over a desired range. The goal of RSM is to produce an n-dimensional surface using a group of techniques in the empirical study of relationships between one or more measured responses and a number of factors. The selection of factors is facilitated by using a method called Design of Experiments (DOE). DOE specifies the factors in orthogonal arrangements to ensure a good spanning of the design space with minimal design input. For example, if a three factor design using three levels for each factor were used, a full factorial DOE requires twenty-seven ship designs to be used as input. Since ship synthesis requires much user interaction and may be difficult to achieve, DOE reduction methods from the full factorial can be used. Two frequently used methods are the Box-Behnken and Central Composite designs. Regardless of the DOE method used to specify factor assignment, the RSM performs a quadratic fit between  $k$  design factors and a response,  $y$ , using the following second degree polynomial approximation:

$$y = b_0 + \sum_{i=1}^k b_i x_i + \sum_{i=1}^k b_{ii} x_i^2 + \sum_{i=1}^k \sum_{j=i+1}^k b_{ij} x_i x_j + \varepsilon. \quad (17)$$

The coefficients  $b_0$ ,  $b_i$ ,  $b_{ii}$ , and  $b_{ij}$  in Equation (17) can be obtained from a multivariate regression software package; the error term,  $\varepsilon$ , represents lack of fit. If the quadratic surface does not accurately fit the data, the design space must be reduced by reducing the range for each factor [6]. The quadratic surface defines a metamodel which can be used in lieu of the ship synthesis model to represent all feasible concept designs.

Current concept exploration methodology is performed by varying design input variables to study effects on output criteria. This *ad hoc* process can take a significant amount of time to complete even a single design, let alone a large number of designs. The goal of RSM is to minimize the number of point designs and ultimately evaluate a design space containing all possible variants within the ranges of the specified input factors. The application of RSM to a design process includes the following three steps:

- Engineering Model: Create a mathematical model of the design and identify the potential factors for each response of interest.
- Screening Experiment: Determine the critical factors that have a statistical impact on the response.
- Response Surface Modeling: Within the design space, create a quadratic surface for the response as a function of the critical factors [6].

In order to create the design space, an engineering model must be available to develop the required number of design variants. There are no readily available synthesis tools for the development of planing boats. There are, however, a few excellent software tools that evaluate planing boat performance. POWERSEA, which was used in Chapter 3 to determine the effects of hull deadrise on vertical acceleration, is an excellent craft motion and resistance predictor. The NAVCAD software package is also a good predictor of resistance, but it is harder to develop hulls with variable deadrise in NAVCAD due to input limitations (only mid-chine deadrise is input). More importantly, NAVCAD is not capable of calculating craft motions. The goal of this project is to analyze the effects of various performance parameters on vertical acceleration in order to minimize shock. Therefore, POWERSEA, which can perform resistance and craft motion predictions, was used as the engineering model for this exercise.

After creating the design space, a screening experiment is typically performed to determine the critical design factors, i.e. those factors which affect the response. A screening experiment that uses DOE is a common method of identifying these factors. The DOE formalizes and systematizes the design process by creating a design space of consistently defined variants. The designer can use statistical analysis to estimate the effect of each factor and their interactions on the response [6]. For the purposes of this project, the critical design factors were designated from the beginning, so a DOE screening experiment was unnecessary. Specifically, hull deadrise was the design factor analyzed in Chapter 3. From previous research, it was determined that hull deadrise might have a significant impact on vertical acceleration. Therefore, hull deadrise was the primary design parameter; the other two design factors considered for this analysis were payload weight and cruise speed. These parameters were adjusted in POWERSEA in order to create the point designs used for the design space.

Once the critical factors are determined and the design space is defined, the response surfaces can be developed. The most common DOE reduction methods are the Box-Behnken and Central Composite designs. The response surface represents all feasible designs within the design space defined by the critical factors. With this response surface, the designer can now examine any point design within the design space without having to create a new design [6].

The Box-Behnken design, which is a three-level, nearly-orthogonal design, is shown in Figure 18 for a three dimensional case.

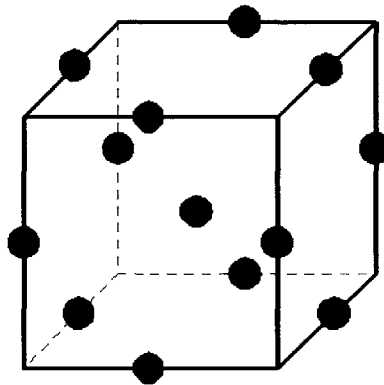


**Figure 18. Box-Behnken Design**

The design space is created from thirteen point designs: one point design is the center point, and the remaining point designs are mid-segment points on the cube. This method estimates main effects, quadratic effects, and simple interactions, but it cannot estimate quadratic interactions. Also, since there are no corner points in this design, there is a higher level of uncertainty near the corner regions. However, the Box-Behnken design is very effective for situations in which the corner points are infeasible [18].

The Central Composite or Box-Wilson design is a three- or five-level design that includes the corner, center, and axial points of the design. The three-factor Central Composite design (CCD) is shown in Figure 19.

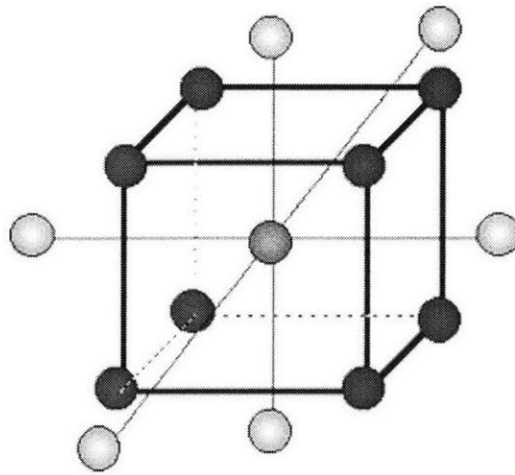


**Figure 19. Central Composite Design**

The three factor design space is developed from 15 point designs: a center point design, eight corner point designs, and 6 axial point designs. This model more accurately represents the response surface since the corner points are included. This model is also useful when screening designs are used, since the screening design inputs can be re-used to help create the Central Composite design space. However, attempting to reach these corner point designs may strain the engineering model [18].

## **4.2 Design Space Creation**

The major focus of this research considered the effects of hull deadrise on vertical acceleration. Therefore, the purpose of the design space study is to analyze the combined effects of hull deadrise and other performance parameters on vertical acceleration. Two major design parameters that affect the vertical motion of a planing boat are payload and speed. Based on the discussion in Chapter 2, the hydrodynamic lift is a determining factor in a planing boat's performance. The speed of the boat determines the lift fraction, and ultimately the displacement. Payload directly affects both speed and displacement. Therefore, a design space encompassing heave acceleration response surfaces based on hull deadrise, cruise speed, and payload will provide all feasible solutions within the specified range of the input parameters.

There are numerous design factors for any given planing boat design. When conducting a preliminary design study, trade-offs are made at every level. The benefit of



using RSM is that the process can identify which design factors affect the various response surfaces, allowing the designer to make adjustments during the early phases of design. A case study that analyzes how different parameters affect a particular response is useful in understanding RSM methodology and is demonstrated in the following sections.

As the engineering model for this analysis is relatively user-friendly, the Central Composite design method was chosen to create the design space. The corner point designs will not stress the model, and these points produce more accurate response surfaces. Table 8 summarizes the design factors used to determine the response surface for vertical acceleration. The -1, 0, and +1 levels represent the low, medium, and high values of each parameter, respectively.

**Table 8. Vertical Acceleration Factor Levels**

<b>Factor (<math>x_i</math>)</b>	<b>-1</b>	<b>0</b>	<b>+1</b>
Mid-chine Deadrise (deg)	24	29	34
Payload Weight (klbs)	0	15	30
Cruise Speed (knots)	30	35	40

JMP, a statistical software package produced by the SAS Institute, was used to create the design space. The JMP DOE specified the fifteen point designs required to create the Central Composite design model. The fifteen variants were created using POWERSEA. Then, calm and rough water simulations were performed to determine vertical acceleration at the Coxswain location. For the rough water simulations, all input conditions with the exception of speed are identical to those described in Table 6 in Chapter 3. All data collected during the simulations that was required to develop the design space is included in Appendix B. Table 9 summarizes the results of the Central Composite design space.

**Table 9. Central Composite Design Summary**

<b>Pattern</b>	<b>Deadrise (deg)</b>	<b>Payload Weight (klbs)</b>	<b>Cruise Speed (kts)</b>	<b>Coxswain Average Heave Acceleration (g)</b>	<b>Coxswain 1/3 Highest Heave Acceleration (g)</b>
++-	34	30	30	0.18	0.74
--+	24	0	40	0.35	1.7
00a	29	15	30	0.23	0.98
+ - +	34	0	40	0.32	1.34
0A0	29	30	35	0.26	1.01
0a0	29	0	35	0.31	1.1
+ --	34	0	30	0.2	0.82
00A	29	15	40	0.34	1.56
+++	34	30	40	0.27	1.25
- ++	24	30	40	0.32	1.22
A00	34	15	35	0.25	0.94
a00	24	15	35	0.28	1.12
---	24	0	30	0.28	1.31
- + -	24	30	30	0.24	1.04
000	29	15	35	0.27	1.27

The pattern defines the coding of the design factors; “+” is high, “-“ is low, “0” is mid-range, “a” is low axial, and “A” is high axial. For example, “+++” represents the corner point design having the highest deadrise (34°), highest payload weight (30 klbs), and highest cruise speed (40 kts).

### **4.3 Design Space Analysis**

The average heave acceleration and 1/3 highest heave acceleration responses were modeled using JMP. The following section discusses some of the pertinent statistical parameters of the responses, evaluates the effects of the design factors on the two responses, and demonstrates the capabilities of JMP with regard to preliminary design of planing boats.

#### **4.3.1 Average Heave Acceleration Response Model**

The data in Table 9 was used to model the average heave acceleration response. Each of the fifteen variants was entered in JMP; standard least squares model fitting was used to obtain a quadratic response surface as a function of the three input factors. This section briefly discusses some of the statistical information determined by JMP; [15]

provides a more detailed understanding of these terms. The leverage plot, which is shown in Figure 20, can be used to examine model fit.

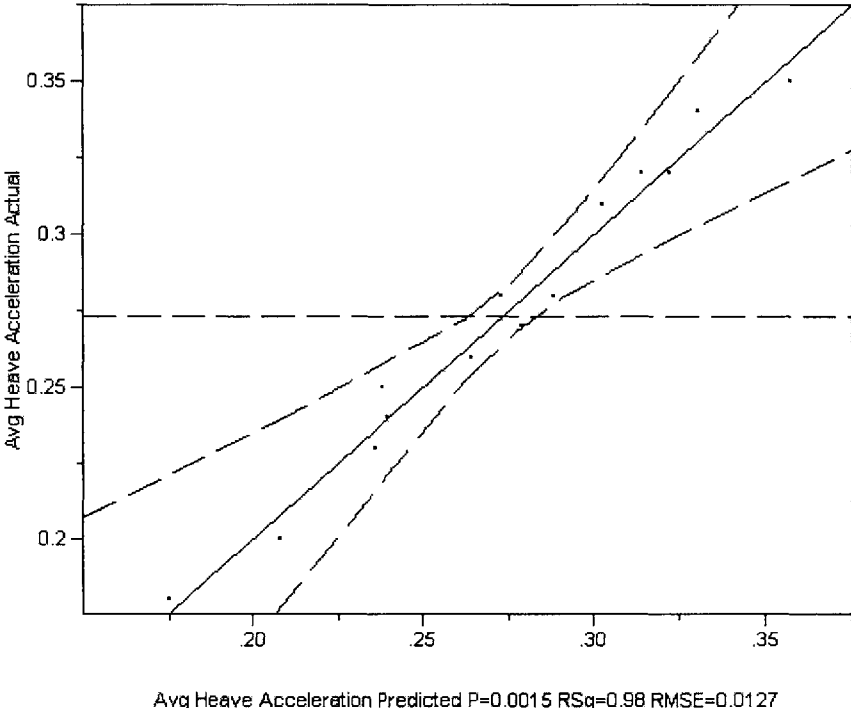


**Figure 20. Average Heave Acceleration Response Model Leverage Plot**

This plot shows the model predicted values (solid line), confidence intervals (dashed lines), and sample mean (horizontal dashed line). The confidence interval graphically shows the 95% confidence region for the line of fit and indicates whether the F Test (to be discussed) is significant at the five percent level. If the confidence curves cross the sample mean, the model is significant; otherwise, the model is not significant at the five percent level. The leverage plot for average heave acceleration clearly illustrates that the model is significant.

The RSq term in the leverage plot estimates the proportion of the variation in average heave acceleration response around the mean that can be attributed to terms in the model rather than to random error. An RSq of 1 describes a perfect fit, an RSq of 0 means the model fit predicts the response no better than the overall response mean. The Root Mean Square Error (RMSE) term estimates the standard deviation of the random error. For the average heave acceleration response, RSq is 0.96, so the model is an excellent fit.

Table 10, the Analysis of Variance, summarizes the quality of the model fit to the actual average heave acceleration response.

**Table 10. Average Heave Acceleration Response Model Analysis of Variance**

Source	DF	Sum of Squares	Mean Square	F Ratio
Model	9	0.03312222	0.003680	22.6865
Error	5	0.00081111	0.000162	Prob > F
C. Total	14	0.03393333		0.0015

The three Sources of variation are Model, Error, and Total. The degrees of freedom (DF) term records an associated DF for each source of variation. The Sum of Squares (SS) terms account for the variability measured in the response. The SS is the sum of squares of the differences between the fitted response and the actual response. The Total Sum of Squares (SS) is the sum of the squared distances from the average heave acceleration response sample mean. The Error SS is the sum of squared differences between the fitted values and the actual values, which corresponds to the unexplained residual Error after fitting the regression model. If the Model SS, the difference between the Total SS and Error SS, is much larger than the Error SS, then the factors accurately model the response. The Mean Square term, which is simply SS divided by DF, converts the SS to an average, and the F Ratio is the model mean square divided by the error mean square. The accuracy of the response is also reflected in the F Ratio, which is used to test the possibility that all coefficients in Equation (17) are zero; the larger the F Ratio, the better the model fit. The “Prob > F” term represents the probability of obtaining a greater F Ratio by chance alone if the model fits no better than the mean of the response. Probabilities of 0.05 or less are normally considered evidence that there is at least one significant regression factor in the model. Since this probability is 0.0015, the model is an excellent predictor of average heave acceleration.

The average heave acceleration coefficients for Equation (17) are shown in Table 11.

**Table 11. Average Heave Acceleration Response Model Coefficients**

Term	Scaled Estimate	Std Error	t Ratio	Prob> t
Intercept	0.2788889	0.006846	40.74	<.0001
Deadrise (deg)(24,34)&RS	-0.025	0.004028	-6.21	0.0016
Payload (klbs)(0,30)&RS	-0.019	0.004028	-4.72	0.0053
Cruise Speed (kts)(30,40)&RS	0.047	0.004028	11.67	<.0001
Deadrise (deg)(24,34)*Payload (klbs)(0,30)	4.441e-16	0.004503	0.00	1.0000
Deadrise (deg)(24,34)*Cruise Speed (kts)(30,40)	0.0075	0.004503	1.67	0.1567
Payload (klbs)(0,30)*Cruise Speed (kts)(30,40)	-0.0025	0.004503	-0.56	0.6027
Deadrise (deg)(24,34)*Deadrise (deg)(24,34)	-0.016111	0.007943	-2.03	0.0983
Payload (klbs)(0,30)*Payload (klbs)(0,30)	0.0038889	0.007943	0.49	0.6451
Cruise Speed (kts)(30,40)*Cruise Speed (kts)(30,40)	0.0038889	0.007943	0.49	0.6451

The standard error is an estimate of the standard deviation for each coefficient. The t Ratio and “Prob > |t|” terms reflect the possibility that each coefficient is zero, similar to the F Ratio. A very large t Ratio indicates that the true coefficient is likely nonzero; the “Prob >|t|” is the probability of generating an even greater t Ratio given that the coefficient is zero. As with the F Ratio, probabilities less than 0.05 typically indicate that the coefficient is nonzero. Table 11 shows that deadrise, payload, and cruise speed are all statistically significant with regard to the average heave acceleration response. As all of the second order effects have “Prob > |t|” greater than 0.05, they are statistically insignificant.

Based on the above discussion, the following conclusions are evident:

- The quadratic model is statistically significant.
- The model can accurately predict average heave acceleration as a function of the three factors with an estimated standard deviation of 0.0127g.
- Cruise speed influences average heave acceleration the most, followed by deadrise and displacement, respectively.

#### 4.3.2 1/3 Highest Heave Acceleration Response

The 1/3 highest heave acceleration response model was created based on the data in Table 9. Figure 21 shows the leverage plot, Table 12 shows the Analysis of Variance, and Table 13 shows the Model Coefficients for the 1/3 highest heave acceleration response model.

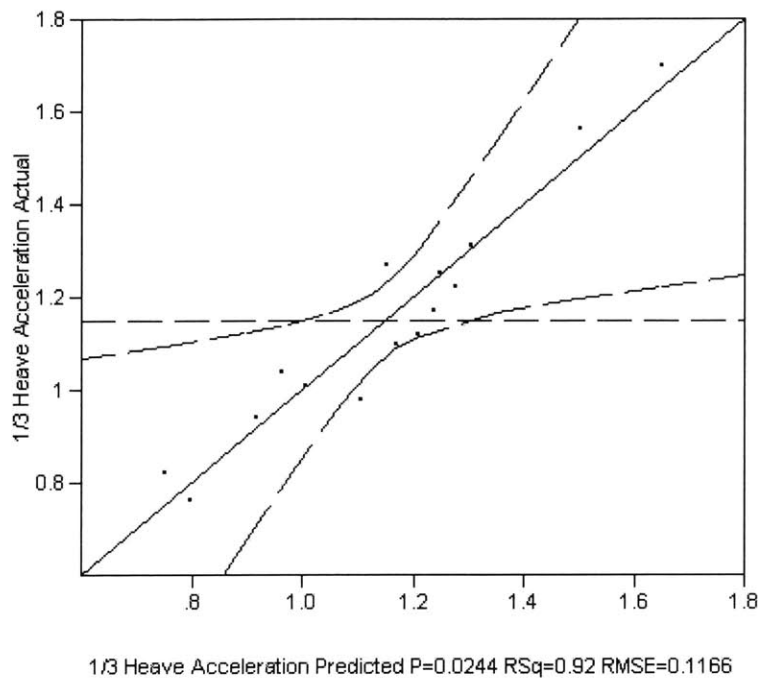


**Figure 21. 1/3 Highest Heave Acceleration Response Model Leverage Plot**

**Table 12. 1/3 Highest Heave Acceleration Response Model Analysis of Variance**

Source	DF	Sum of Squares	Mean Square	F Ratio
Model	9	0.82699306	0.091888	6.7558
Error	5	0.06800694	0.013601	Prob > F
C. Total	14	0.89500000		0.0244

**Table 13. 1/3 Highest Heave Acceleration Response Model Coefficients**

Term	Scaled Estimate	Std Error	t Ratio	Prob> t
Intercept	1.1477778	0.062684	18.31	<.0001
Deadrise (deg)(24,34)&RS	-0.145	0.03688	-3.93	0.0111
Payload (klbs)(0,30)&RS	-0.082	0.03688	-2.22	0.0768
Cruise Speed (kts)(30,40)&RS	0.199	0.03688	5.40	0.0030
Deadrise (deg)(24,34)*Payload (klbs)(0,30)	0.09625	0.041233	2.33	0.0669
Deadrise (deg)(24,34)*Cruise Speed (kts)(30,40)	0.03375	0.041233	0.82	0.4503
Payload (klbs)(0,30)*Cruise Speed (kts)(30,40)	-0.00875	0.041233	-0.21	0.8403
Deadrise (deg)(24,34)*Deadrise (deg)(24,34)	-0.087222	0.072728	-1.20	0.2841
Payload (klbs)(0,30)*Payload (klbs)(0,30)	-0.062222	0.072728	-0.86	0.4313
Cruise Speed (kts)(30,40)*Cruise Speed (kts)(30,40)	0.1527778	0.072728	2.10	0.0897

With an RSq value of 0.92 and a Prob > F of 0.0244, this model is also an excellent fit.

The Prob > |t| for deadrise and cruise speed is less than 0.05, so each of these parameters is statistically significant with regard to the 1/3 highest heave acceleration response.

However, the payload has a Prob > |t| of 0.0768, so payload does not statistically influence the 1/3 highest heave acceleration response.

The following conclusions can be drawn from the 1/3 highest heave acceleration response analysis:

- The quadratic model is statistically significant.
- The model can accurately predict 1/3 highest heave acceleration as a function of the three factors with an estimated standard deviation of 0.1166g.
- Cruise speed influences 1/3 highest heave acceleration the most, deadrise has a significant but lesser affect, and payload does not statistically affect the response.

### **4.3.3 Design Space Case Studies**

The capabilities of JMP have only been touched upon thus far. The tool is most useful in a visual demonstration, as decisions made by a designer can be analyzed, changed, and re-analyzed with a few keystrokes. That is the power of RSM: trade-offs can be made instantaneously without having to perform lengthy design syntheses. Some of the pertinent JMP graphics will be presented in the following section to best capture this dynamic process. The purpose of this section is to demonstrate the applicability of RSM to preliminary, top-level planing boat design. Two case studies are performed to analyze planing boats when vertical acceleration is a design factor. Case 1 will concern setting operational limits for an existing boat design, and Case 2 will consider preliminary design of a new planing boat.

While the MkV SOC has excellent performance characteristics with regard to speed, range, and payload, it has been shown to be an uncomfortable ride due to the numerous mechanical shock events encountered during normal operations. Research on shock mitigation is dominated by short-term, bolt-on solutions that can be implemented as soon as possible. The following analysis shows how changes in cruise speed and payload affect vertical accelerations.

The design space created in the preceding section varied deadrise, payload, and cruise speed. For this example, deadrise will remain fixed at the baseline level of 29°,

and trade-offs in cruise speed and payload will be studied to determine possible operating envelopes. Figure 22 shows the complete design space qualitatively for a fixed deadrise of 29°.

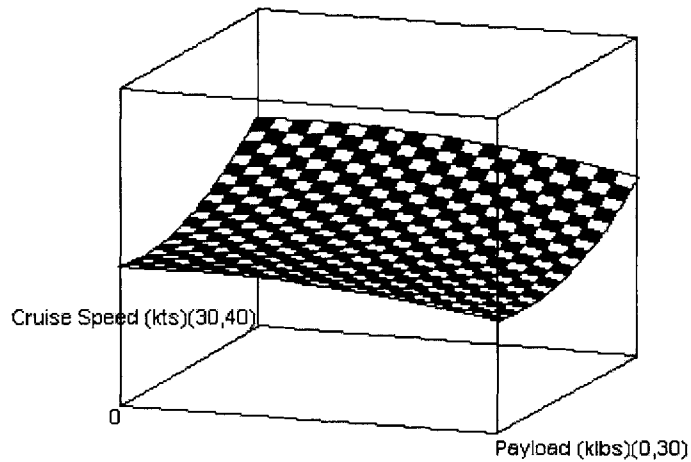


**Figure 22. Case 1 Heave Acceleration vs. Cruise Speed and Payload**

For any combination of cruise speed and payload, the predicted value of 1/3 highest heave acceleration can be determined. As determined in the previous section, the combination of highest payload and lowest speed produces the lowest 1/3 highest heave acceleration.

Figure 23 shows the contour profile for 1/3 highest heave acceleration assuming a fixed deadrise of 29°.



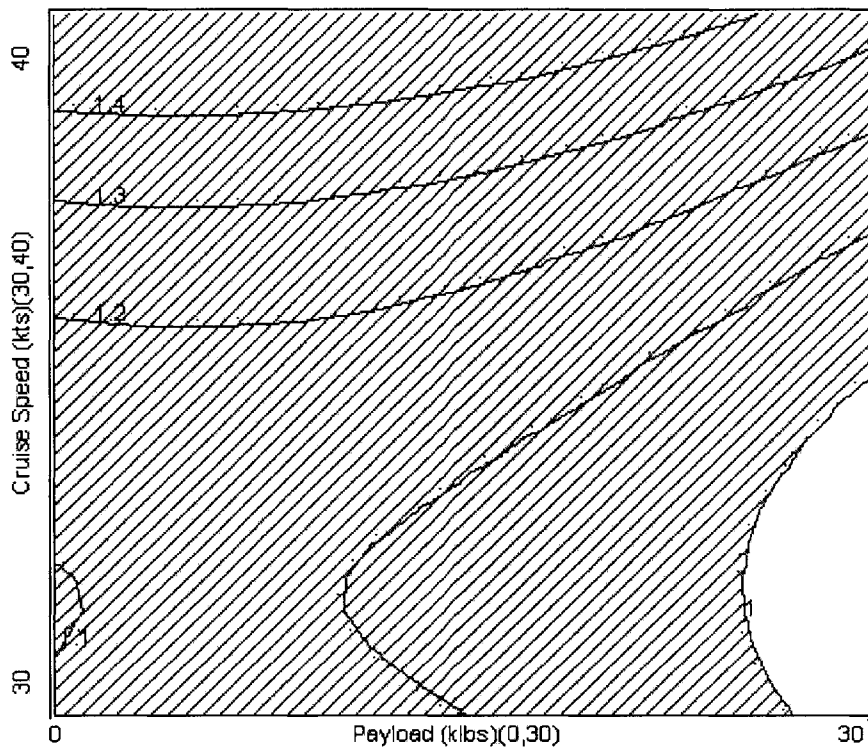


**Figure 23. Case 1 Heave Acceleration Contour Profile**

Each contour line represents a constant value of 1/3 highest heave acceleration. This plot can be used to determine the operating conditions required to ensure vertical accelerations below a specified level. For example, if the upper limit on vertical acceleration (for the specified sea conditions) was 1g, the only possible combinations of speed and payload are those in the unshaded region of the plot, below and to the right of the 1g contour. Any combination of cruise speed and payload can be specified to determine the corresponding 1/3 highest heave acceleration, or a 1/3 highest heave acceleration can be specified to determine the possible ranges of cruise speed and payload. Again, it must be emphasized that no additional design work is required to make these determinations; once the work of creating the point designs is finished, trade-off comparisons can be made instantly.

Perhaps the most beneficial use of RSM is during the early phases of preliminary design. Case 2 assumes that the ranges for deadrise, payload, and cruise speed have been narrowed to the ranges specified in Table 8. Assuming that vertical acceleration is a

design criterion, the JMP analysis performed in the previous section can be used to evaluate all feasible designs in this design space. Of course, vertical acceleration is only one of many responses that the designer will need, but for the purpose of this exercise, it is assumed that it is the only response being considered.

The two factors that affect the 1/3 highest heave acceleration the most are cruise speed and hull deadrise. Figure 24 shows the contour profile for a fixed payload of fifteen thousand pounds and variable speed and deadrise.

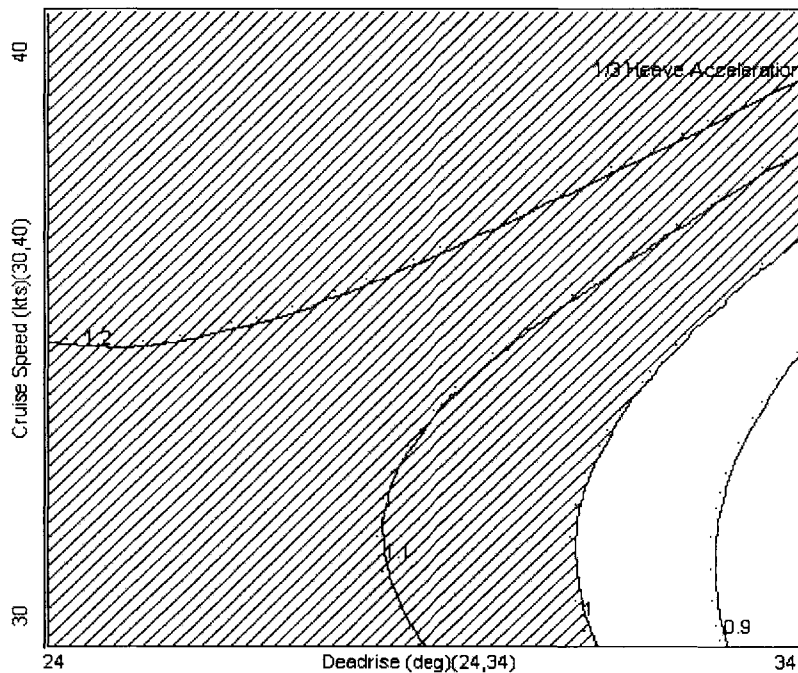


**Figure 24. Case 2 Contour Profile (15 klbs Payload)**

The contours show the combinations of deadrise and cruise speed required to produce the specified vertical acceleration. For an upper limit of 1g, only combinations of high deadrise and low cruise speed produce a satisfactory response (unshaded region).

Figure 25 shows the same contours but for a fixed payload of thirty thousand pounds and assumed heave acceleration limit of 1g..

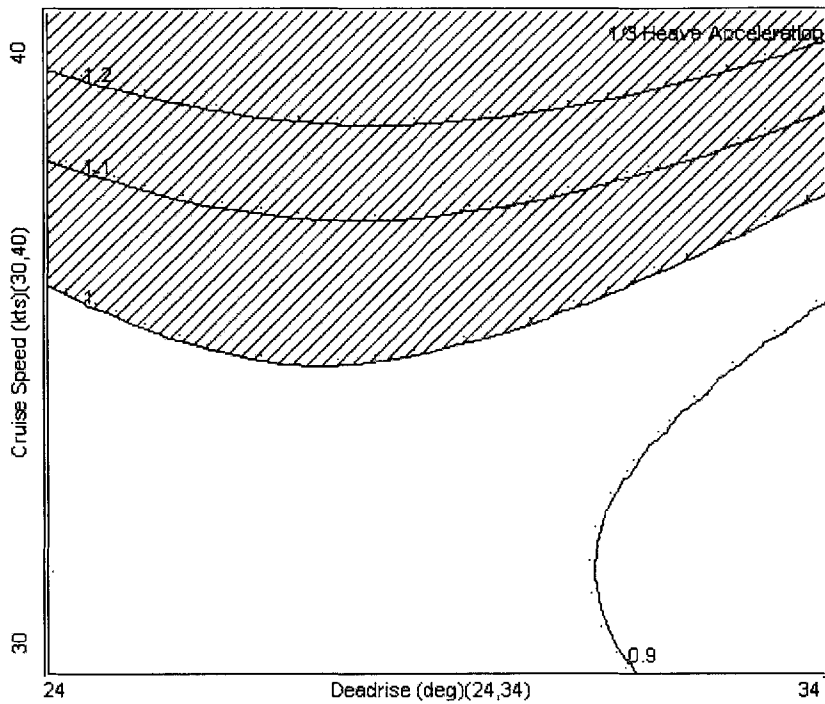


**Figure 25. Case 2 Contour Profile (30 klbs Payload)**

For the higher value of payload weight, the region of possible designs in the unshaded region is much larger. The design deadrise can be any value within the specified range; the designer can therefore optimize the design for cruise speed. In this case, the highest possible deadrise of 34 produces a maximum cruise speed of 37.2 knots. This greater flexibility is crucial in the early stages of design.

# Chapter 5

## Conclusions

The correlation between Naval Special Warfare high speed planing boat operation and injury is well-documented. Current solutions focus on bolt-on solutions that can be implemented on existing boats, i.e. placing new suspension seats on the MkV SOC. This thesis examines a long-term shock mitigation solution by determining the relationship between hull deadrise and a planing boat's vertical acceleration. Hull deadrise does indeed influence these accelerations and should be analyzed in more detail during next-generation planing boat design. Furthermore, two case studies show how future designs can incorporate Response Surface Methods in preliminary design to optimize a planing boat design for shock mitigation purposes.

### 5.1 Optimal Deadrise Hull Analysis

The POWERSEA Time-Domain Planing Hull Simulation software was used to study the effects of hull deadrise on vertical acceleration. A baseline MkV SOC hull was created and compared to at-sea craft motion tests. Twenty-five additional hulls having the same overall length and beam of the MkV SOC were created; deadrise was varied from fifteen degrees below to ten degrees above the baseline deadrise. Calm and rough water simulations were performed to determine the resistance and heave acceleration of each hull. The ODH results show that an increase in hull deadrise of only six percent can reduce a boat's average heave acceleration by twenty percent and 1/3 highest heave acceleration by twenty-three percent with no loss in performance. An increase in hull deadrise in a future design, combined with some type of suspension seating and cockpit isolation, will likely produce the most effective shock mitigation system.

## 5.2 Design Space Study

RSM was used to develop a Central Composite design space using fifteen design variants. Each variant has a different combination of three design factors: deadrise, cruise speed, and payload weight. The design space, which was created with the aid of the JMP Statistical Discovery Software package, allows the designer to examine all feasible designs within the space as part of a multiple criteria decision making process. An analysis of the design space showed that both average and 1/3 highest heave acceleration responses can be modeled accurately and that these models are most influenced by cruise speed, hull deadrise, and payload weight, in that order.

Two case studies were performed to demonstrate the applicability of RSM to planing boat design. Case 1 showed that operational limits can be determined for an existing planing boat design by examining the combined effects of cruise speed and payload on vertical acceleration. Case 2 argued that RSM can reduce planing boat heave accelerations and subsequently reduce mechanical shock when implemented early in the design process. By analyzing the complete design space, the designer can examine all feasible concept designs within the design space, without having to perform lengthy design syntheses. In summary, RSM can accomplish the following:

- For the selected response, the designer can examine an infinite number of combinations of the design factors to determine the combined effect on the response. The response surface can help the designer determine which factors have a significant impact on the response and ultimately enables the designer to focus on these critical factors.
- The designer can perform a trade-off study to determine how selection of one or more factors limits the selection of the remaining factors.
- By setting limits on the response, the designer can reduce the feasible design space and determine whether a solution is possible for the specified response.

## 5.3 Recommendations for Future Work

This thesis examines the impact of hull deadrise on planing boat vertical acceleration and creates a design space to determine the combined affects of deadrise,

cruise speed, and payload weight on these accelerations. To improve upon this work, future research is required in several areas.

First and foremost, the deadrise analysis must be performed with the specific boat geometry. Due to proprietary reasons, the hull and station offsets of the MkV SOC were unavailable for use during the course of this research. The overall length and maximum beam of the vessel were known, however, so a relatively accurate model of the boat was developed for simulation purposes. In any case, the results of this thesis unmistakably show that there is a relationship between a boat's vertical acceleration and its deadrise.

Although POWERSEA is an excellent analysis tool, a synthesis tool should be used in the future to more accurately represent the various parameters derived from a planing boat's geometry. Specifically, changes in hull deadrise result in changes in a vessel's displacement and radius of gyration. These two parameters were held constant for all analyses performed in Chapter 3. The radius of gyration is not significantly affected by changes in deadrise, as the length and beam of the boat were held constant, and the changes in displacement are negligible for small changes in deadrise. Regardless, a complete synthesis of each hull form will eliminate any uncertainty in the results.

For next-generation boat design, some measurable limit must be developed for human exposure to shock in order to develop an optimal hull form for vertical acceleration. While smaller magnitude and shorter pulse shock events are certainly better, an effective design can only be as good as the criteria it is measured against. Additionally, boat geometry limits must be delineated in order to evaluate all feasible hulls. Should the MkV SOC transportation requirements remain in affect, the general dimensions are limited, as discussed in Chapter 3.

Finally, all factors influencing planing boat vertical acceleration must be identified. A design of experiments can be used to determine the critical factors that statistically affect the response, and response surface methods can be used to model the complete design space. In order to optimize the overall design, responses other than vertical acceleration should be determined. Ideally, an Overall Measure of Effectiveness Model can be developed to prioritize the various responses based on NSW community input. Ultimately, a trade-off study can be performed to determine the global effects of changes in the critical design factors.

# **Appendix A**

## **POWERSEA ODH Data**

Forebody Deadrise (deg)	Mid-chine Deadrise (deg)	Resistance at 35 kts (Hp)		Heave Loc (feet)	Pitch (deg)	CG Heave Accel (g)	Coxswain Heave Accel (g)
19.5	15	1307.3	Min	-0.1884	-0.1005	-0.5056	0.0033
			Mean	0.7795	2.1997	-0.0003	0.3325
			Max	1.7620	5.1120	2.1048	3.2804
			Std Dev	0.4185	1.0852	0.3053	0.3289
			Max Ht	1.8868	5.1270	2.4992	3.1966
			H(1/3)	1.5894	4.6376	2.4556	2.3531
20.8	16	1332.1	Min	-0.3515	-0.2162	-0.4685	0.0041
			Mean	0.6897	2.1581	-0.0024	0.3197
			Max	1.5446	4.9385	1.3200	2.2076
			Std Dev	0.4080	1.1261	0.2736	0.2813
			Max Ht	1.7568	5.0140	1.7885	2.1984
			H(1/3)	1.4998	4.5590	1.9649	1.8318
21.7	17	1355.9	Min	-0.3318	-0.3246	-0.5060	0.0009
			Mean	0.5961	2.1781	-0.0005	0.3279
			Max	1.5319	4.8944	2.8049	4.3484
			Std Dev	0.3796	1.0207	0.2935	0.3207
			Max Ht	1.7520	4.7321	3.3109	4.2902
			H(1/3)	1.4457	3.7770	2.2044	2.0973
22.2	18	1390	Min	-0.3597	-0.0434	-0.5404	0.0021
			Mean	0.4626	2.0150	-0.0037	0.2818
			Max	1.5789	5.4120	1.3426	2.2240
			Std Dev	0.3711	1.0656	0.2504	0.2848
			Max Ht	1.8342	5.3530	1.8391	2.0481
			H(1/3)	1.5633	4.9012	1.9388	2.0208
23.1	19	1410.6	Min	-0.5179	-0.5258	-0.5113	0.0039
			Mean	0.3987	2.0350	-0.0000	0.3259
			Max	1.9201	6.6130	1.4944	2.3853
			Std Dev	0.3971	1.1378	0.2756	0.3019
			Max Ht	2.4380	7.1390	1.9623	2.3814
			H(1/3)	1.6908	4.4233	2.0335	2.0302
24.3	20	1439.5	Min	-0.7512	-0.7212	-0.5031	0.0021
			Mean	0.3147	2.0344	-0.0039	0.3145
			Max	1.4312	5.4800	1.8619	3.0260
			Std Dev	0.3996	1.1922	0.2742	0.3104
			Max Ht	1.9372	6.2010	2.3651	2.9671
			H(1/3)	1.6824	5.2210	1.9610	2.2598
26	21	1453.2	Min	-0.9589	-0.8495	-0.4997	0.0010
			Mean	0.1776	1.9549	-0.0004	0.3014
			Max	1.2166	5.4170	1.4629	2.4316
			Std Dev	0.3862	1.1463	0.2525	0.2711
			Max Ht	2.1756	6.2300	1.9166	2.4186
			H(1/3)	1.5992	4.7882	1.6546	1.7706



Forebody Deadrise (deg)	Mid-chine Deadrise (deg)	Resistance at 35 kts (Hp)		Heave Loc (feet)	Pitch (deg)	CG Heave Accel (g)	Coxswain Heave Accel (g)
28.4	22	1450.5	Min	-0.9790	-1.1002	-0.5184	0.0009
			Mean	0.0670	1.9730	0.0013	0.2861
			Max	1.2796	5.0520	1.3634	2.1038
			Std Dev	0.3956	1.1787	0.2372	0.2503
			Max Ht	2.0454	5.7510	1.8254	2.0718
			H(1/3)	1.5910	4.7315	1.5027	1.5387
28.8	23	1485.9	Min	-1.1619	-1.4538	-0.4963	0.0004
			Mean	-0.0138	1.9412	-0.0005	0.2986
			Max	1.4941	6.7300	1.1240	2.1215
			Std Dev	0.4004	1.2094	0.2425	0.2658
			Max Ht	2.5626	7.5540	1.6203	2.0991
			H(1/3)	1.5577	5.0110	1.4157	1.5737
31.1	24	1513.8	Min	-1.1863	-0.7981	-0.5304	0.0013
			Mean	-0.1633	1.8259	-0.0019	0.2826
			Max	1.0663	4.9079	1.3056	2.0528
			Std Dev	0.3805	1.1284	0.2222	0.2208
			Max Ht	1.9776	5.3850	1.8360	2.0336
			H(1/3)	1.3982	4.4506	1.3034	1.2583
33.1	25	1522.8	Min	-1.1307	-0.6424	-0.5071	0.0008
			Mean	-0.2798	1.8379	0.0019	0.2743
			Max	0.7621	5.1050	1.4744	2.3314
			Std Dev	0.3846	1.1336	0.2208	0.2281
			Max Ht	1.8620	5.7030	1.8380	2.2668
			H(1/3)	1.5721	4.4878	1.2710	1.2804
33.5	26	1560.7	Min	-1.2559	-1.2331	-0.5228	0.0009
			Mean	-0.3794	1.7496	-0.0013	0.2715
			Max	0.6823	4.9084	0.8795	1.4884
			Std Dev	0.3732	1.1462	0.2125	0.2195
			Max Ht	1.7845	5.8130	1.3644	1.3985
			H(1/3)	1.6357	4.7621	1.1367	1.1479
33.9	27	1594.3	Min	-1.3818	-0.6937	-0.5776	0.0020
			Mean	-0.4910	1.6650	0.0010	0.2800
			Max	0.4935	5.1390	0.9162	1.4881
			Std Dev	0.3823	1.1879	0.2073	0.1993
			Max Ht	1.8629	5.8330	1.3078	1.4485
			H(1/3)	1.5483	5.0360	0.9893	0.9702
34.1	28	1632.1	Min	-1.6622	-1.0235	-0.5640	0.0015
			Mean	-0.5812	1.5570	-0.0002	0.2688
			Max	0.7460	5.7910	0.7174	1.3833
			Std Dev	0.3743	1.1547	0.2068	0.2180
			Max Ht	2.1999	6.6100	1.2770	1.3172
			H(1/3)	1.8270	5.1940	1.0564	1.1550

Forebody Deadrise (deg)	Mid-chine Deadrise (deg)	Resistance at 35 kts (Hp)		Heave Loc (feet)	Pitch (deg)	CG Heave Accel (g)	Coxswain Heave Accel (g)
34.5	29	1661.3	Min	-1.8824	-1.6729	-0.6599	0.0011
			Mean	-0.6899	1.4519	-0.0019	0.2646
			Max	0.7765	6.1860	0.9606	1.6087
			Std Dev	0.3803	1.2642	0.2002	0.2011
			Max Ht	2.6589	7.8590	1.6204	1.5891
			H(1/3)	1.6043	5.2430	0.9433	1.0098
34.8	30	1689.6	Min	-1.6345	-1.3517	-0.5866	0.0004
			Mean	-0.7822	1.5745	0.0005	0.2413
			Max	0.6681	4.9346	0.6719	1.2206
			Std Dev	0.3911	1.0432	0.1888	0.1776
			Max Ht	2.3027	5.6950	1.2299	1.1737
			H(1/3)	1.6712	3.8970	0.8669	0.8889
35.2	31	1714.3	Min	-1.8989	-0.9800	-0.4572	0.0034
			Mean	-0.8850	1.5045	0.0018	0.2233
			Max	0.2459	3.9300	0.6039	1.0058
			Std Dev	0.4180	1.0247	0.1804	0.1621
			Max Ht	2.1246	4.7595	0.9285	0.9512
			H(1/3)	1.7163	3.9832	0.8234	0.8117
35.6	32	1646.3	Min	-1.8789	-1.0205	-0.4350	0.0015
			Mean	-0.9751	1.4666	-0.0017	0.2188
			Max	0.2317	4.5090	0.5630	1.0226
			Std Dev	0.3995	1.0507	0.1731	0.1637
			Max Ht	2.1106	5.1950	0.9379	0.9814
			H(1/3)	1.6033	4.0988	0.7871	0.8257
37.5	33	1601.3	Min	-2.0008	-1.4034	-0.5183	0.0032
			Mean	-1.1412	1.3036	-0.0013	0.2374
			Max	-0.2681	4.1315	0.6196	1.1289
			Std Dev	0.3527	1.1657	0.1735	0.1773
			Max Ht	1.6543	5.5350	1.0387	1.0865
			H(1/3)	1.4112	4.7585	0.8674	0.9206
38	34	1616.8	Min	-2.1696	-2.2475	-0.4546	0.0037
			Mean	-1.2584	1.2681	0.0041	0.2314
			Max	-0.1755	4.7589	0.9945	1.3879
			Std Dev	0.3565	1.1755	0.1820	0.2054
			Max Ht	1.9941	7.0060	1.3420	1.2604
			H(1/3)	1.4359	5.1800	0.8583	0.9203
39	35	1614.1	Min	-2.2810	-2.1591	-0.4926	0.0037
			Mean	-1.3907	1.2036	-0.0008	0.2083
			Max	-0.3734	4.7873	0.4365	0.8175
			Std Dev	0.3399	1.1456	0.1554	0.1612
			Max Ht	1.8519	6.9460	0.9118	0.7686
			H(1/3)	1.3778	5.1970	0.6588	0.7756

Forebody Deadrise (deg)	Mid-chine Deadrise (deg)	Resistance at 35 kts (Hp)		Heave Loc (feet)	Pitch (deg)	CG Heave Accel (g)	Coxswain Heave Accel (g)
40	36	1618.8	Min	-2.4537	-1.3665	-0.4471	0.0019
			Mean	-1.5028	1.1438	-0.0006	0.2100
			Max	-0.6454	4.5102	0.6340	1.2134
			Std Dev	0.3641	1.1505	0.1576	0.1589
			Max Ht	1.6816	5.8770	1.0685	1.1603
			H(1/3)	1.4112	4.7739	0.7313	0.8267
41	37	1620.4	Min	-2.5470	-1.2582	-0.3757	0.0015
			Mean	-1.6492	1.0416	-0.0025	0.2072
			Max	-0.6998	4.2170	0.5366	0.9276
			Std Dev	0.3597	1.1434	0.1537	0.1498
			Max Ht	1.8072	5.4750	0.8944	0.8740
			H(1/3)	1.4766	4.9096	0.6768	0.7166
42	38	1610	Min	-2.5705	-2.0026	-0.5885	0.0029
			Mean	-1.8062	0.9405	0.0008	0.1983
			Max	-0.7204	4.2106	0.5169	1.1275
			Std Dev	0.3297	1.1043	0.1462	0.1514
			Max Ht	1.7308	6.2130	1.1054	1.0145
			H(1/3)	1.4966	4.5708	0.5797	0.7102
43	39	1599.9	Min	-2.9636	-1.8103	-0.4132	0.0013
			Mean	-1.9388	0.8596	-0.0011	0.1980
			Max	-1.0669	4.1287	0.5891	1.0232
			Std Dev	0.3767	1.2189	0.1503	0.1549
			Max Ht	1.8195	5.8630	0.9467	0.9869
			H(1/3)	1.4454	5.1790	0.6835	0.8021
44	40	1597.5	Min	-3.0434	-2.4658	-0.4542	0.0024
			Mean	-2.0393	0.7738	-0.0001	0.1827
			Max	-0.7484	4.4909	0.3742	0.7242
			Std Dev	0.4096	1.1978	0.1498	0.1489
			Max Ht	2.1478	6.6710	0.7959	0.6526
			H(1/3)	1.9828	5.5530	0.5439	0.7176

# **Appendix B**

## **POWERSEA Design Space Data**

Row	Pattern		Heave Loc (feet)	Pitch (deg)	Heave Accel (g)	Coxswain Heave Accel (g)
1	++-	Min	-2.4550	-1.6852	-0.4475	0.0019
		Mean	-1.5178	0.9805	-0.0018	0.1910
		Max	-0.4126	4.3064	0.6781	1.1617
		Std Dev	0.3983	1.1698	0.1478	0.1474
		Max Ht	2.0424	5.9920	1.1256	1.0817
		H(1/3)	1.7459	4.5831	0.6856	0.7567
2	--+	Min	-0.5448	-1.6043	-0.6736	0.0015
		Mean	0.3702	1.3474	0.0007	0.3528
		Max	1.6787	5.6270	1.6350	2.5149
		Std Dev	0.4067	1.2667	0.2779	0.2854
		Max Ht	2.0983	6.8160	2.2281	2.4589
		H(1/3)	1.7577	5.3100	1.7101	1.7000
3	00a	Min	-1.6792	-1.7638	-0.4891	0.0011
		Mean	-0.7275	1.0018	-0.0008	0.2264
		Max	0.4733	5.4210	0.6206	1.0591
		Std Dev	0.3708	1.2863	0.1687	0.1744
		Max Ht	2.1525	6.9090	1.0754	1.0144
		H(1/3)	1.5255	5.4910	0.8764	0.9815
4	+++	Min	-1.4157	-2.2417	-0.6718	0.0009
		Mean	-0.5379	1.0122	-0.0011	0.2904
		Max	0.5460	5.0660	0.7772	1.5160
		Std Dev	0.3319	1.2538	0.2091	0.2260
		Max Ht	1.9617	7.2840	1.3754	1.4646
		H(1/3)	1.4324	5.3010	1.0173	1.1741
5	0A0	Min	-1.8824	-1.6729	-0.6599	0.0011
		Mean	-0.6899	1.4519	-0.0019	0.2646
		Max	0.7765	6.1860	0.9606	1.6087
		Std Dev	0.3803	1.2642	0.2002	0.2011
		Max Ht	2.6589	7.8590	1.6204	1.5891
		H(1/3)	1.6043	5.2430	0.9433	1.0098
6	0a0	Min	-1.1314	-1.8642	-0.5991	0.0024
		Mean	-0.2798	0.8789	0.0079	0.3134
		Max	0.9320	4.5050	0.9418	1.5436
		Std Dev	0.3655	1.3154	0.2295	0.2275
		Max Ht	1.9910	5.9450	1.4573	1.5104
		H(1/3)	1.5475	5.4750	1.1153	1.0950

Row	Pattern		Heave Loc (feet)	Pitch (deg)	Heave Accel (g)	Coxswain Heave Accel (g)
7	+--	Min	-1.7639	-3.0394	-0.5682	0.0009
		Mean	-0.9707	0.3375	-0.0016	0.2031
		Max	0.0096	5.0090	0.4170	0.8195
		Std Dev	0.3468	1.3669	0.1428	0.1616
		Max Ht	1.7159	8.0490	0.9757	0.7871
		H(1/3)	1.6367	5.6660	0.6424	0.8224
8	00A	Min	-1.2273	-1.7337	-0.6628	0.0009
		Mean	-0.2576	1.4513	-0.0020	0.3407
		Max	1.0198	5.9610	1.1861	1.9617
		Std Dev	0.4014	1.3380	0.2538	0.2682
		Max Ht	2.2060	7.6950	1.6981	1.9446
		H(1/3)	1.7840	5.7730	1.3246	1.5649
9	+++	Min	-1.7809	-0.8034	-0.6201	0.0024
		Mean	-0.9767	1.5540	0.0002	0.2657
		Max	0.1035	4.7937	1.3305	2.2472
		Std Dev	0.3413	1.0779	0.2066	0.2341
		Max Ht	1.8844	5.5820	1.9140	2.1711
		H(1/3)	1.6328	4.6901	1.0883	1.2498
10	-++	Min	-0.8580	-0.9422	-0.5583	0.0021
		Mean	0.0601	1.8908	0.0004	0.3195
		Max	1.2426	4.9989	0.9589	1.6342
		Std Dev	0.3744	1.0820	0.2471	0.2363
		Max Ht	1.9753	5.6820	1.3717	1.5529
		H(1/3)	1.5697	4.4721	1.2351	1.2176
11	A00	Min	-1.8452	-1.6790	-0.5503	0.0007
		Mean	-1.0138	0.9773	-0.0001	0.2455
		Max	0.1729	5.2750	0.7547	1.3681
		Std Dev	0.3364	1.2696	0.1759	0.1921
		Max Ht	1.7892	6.7500	1.2140	1.3538
		H(1/3)	1.3403	5.2330	0.8112	0.9387
12	a00	Min	-0.7921	-1.8750	-0.5988	0.0005
		Mean	0.0039	1.5386	0.0010	0.2846
		Max	1.2714	5.3250	1.2333	1.9762
		Std Dev	0.3889	1.2274	0.2232	0.2285
		Max Ht	2.0635	6.9220	1.6777	1.9020
		H(1/3)	1.6042	5.3190	1.1359	1.1211

Row	Pattern		Heave Loc (feet)	Pitch (deg)	Heave Accel (g)	Coxswain Heave Accel (g)
13	---	Min	-1.2293	-2.8636	-0.4894	0.0023
		Mean	-0.0024	0.9515	0.0146	0.2780
		Max	1.3124	5.2810	0.9069	1.5899
		Std Dev	0.3889	1.2963	0.2184	0.2338
		Max Ht	2.5416	8.1440	1.3667	1.4866
		H(1/3)	1.5962	5.3560	1.2024	1.3138
14	-+-	Min	-1.2340	-0.6970	-0.4943	0.0016
		Mean	-0.4161	1.7409	0.0018	0.2357
		Max	0.7213	5.4240	0.8127	1.3286
		Std Dev	0.3530	1.0802	0.1883	0.1961
		Max Ht	1.9450	4.5275	1.2437	1.2878
		H(1/3)	1.4538	3.7787	0.9731	1.0368
15	000	Min	-1.4557	-1.7271	-0.6845	0.0033
		Mean	-0.4947	1.2717	-0.0033	0.2736
		Max	0.9864	5.4230	0.8756	1.4501
		Std Dev	0.3786	1.2857	0.2085	0.2225
		Max Ht	2.4064	6.4830	1.5300	1.4319
		H(1/3)	1.6166	5.3400	1.1007	1.2659

# References

- [1] Akers, Richard H., "Dynamic Analysis of Planing Boats in the Vertical Plane," presented to the New England Section of the Society of Naval Architects and Marine Engineers, April 1999.
- [2] Commander Naval Special Warfare Command, "Missions and History," [Online document], [cited May 3, 2002], Available HTTP: <https://www.navsoc.navy.mil/history.htm>.
- [3] Commander Special Boat Squadron 1, "Mk V Suspended Seat Evaluation," Feb. 2002.
- [4] Federation of American Scientists, "Mark V Special Operations Craft," [Online document], Dec. 1998, Available HTTP: [http://www.fas.org/man/dod-101/sys/ship/mark\\_v.htm](http://www.fas.org/man/dod-101/sys/ship/mark_v.htm).
- [5] Gillmer, Thomas C. and Bruce Johnson, Introduction to Naval Architecture, Naval Institute Press, 1982.
- [6] Goggins, David A., "Response Surface Methods Applied to Submarine Design," Master's Thesis, Massachusetts Institute of Technology, Sept. 2001.
- [7] Hadler, J. B., "The Prediction of Power Performance on Planing Craft," Society of Naval Architects and Marine Engineers *Transactions*, Vol. 74, 1966.
- [8] Haupt, Kelly D., "MKVSOC951 Craft Motions Test Results," Naval Surface Warfare Center, Carderock Division, October 1996.
- [9] Kausel, Eduardo and Jose Manuel Roesset, "Advanced Structural Dynamics," NPI, 2001.
- [10] Kearns, Sean D., "Analysis and Mitigation of Mechanical Shock Effects on High Speed Planing Boats," Master's Thesis, Massachusetts Institute of Technology, Sept. 2001.
- [11] Lewis, Edward V. (ed.), Principles of Naval Architecture, Society of Naval Architects and Marine Engineers, 1988



- [12] Peterson, Ronald, David Wyman and Carolyn Frank, "Drop Tests to Support Water Impact and Planing Boat Dynamics Theory," CSS/TR-97/25, Coastal Systems Station, Dahlgren Division Naval Surface Warfare Center, Panama City, FL, Sept. 1997.
- [13] Peterson, Ronald and R. Gollwitzer, "Shock Mitigation for HSPBs," Coastal Systems Station, Dahlgren Division, Naval Surface Warfare Center, Panama City, FL, Dec. 2000.
- [14] Prusaczyk, Keith W., "Biomedical Aspects of NSW Special Boat Operations," Office of Naval Research, 2000.
- [15] SAS Institute, JMP Statistical Discovery Software User's Manuals, 2000.
- [16] Savitsky, Daniel, "Hydrodynamic Design of Planing Hulls," Marine Technology, Vol. 1, No. 1, Society of Naval Architects and Marine Engineers, 1964.
- [17] Savitsky, Daniel and P. Ward Brown, "Procedures for Hydrodynamic Evaluation of Planing Hulls in Smooth and Rough Water," Marine Technology, Vol. 13, No. 4, Society of Naval Architects and Marine Engineers, 1976.
- [18] Schmidt, Stephen R. and Robert G. Launsby, Understanding Industrial Experiments, Air Academy Press and Associates, 4<sup>th</sup> edition, 1988.
- [19] von Gierke, Henning E. and Anthony J. Brammer, Shock and Vibration Handbook, Fourth Edition, ed. Cyril M. Harris, McGraw-Hill, New York, 1999.
- [20] von Karman, Theodore, "The Impact of Seaplane Floats during Landing," NACA Technical Note 321, 1929.
- [21] Vorus, William S. and Richard Royce, "Wave Impact Reduction of Planing Boats," University of New Orleans, 1999.
- [22] Zhao, R., O. Faltinsen and J. Aarsnes, "Water Entry of Arbitrary Two-Dimensional Section With and Without Flow Separation," 21<sup>st</sup> Symposium on Naval Hydrodynamics, Trondheim, Norway, 1996.